Brain-behavior patterns define a dimensional biotype in medication-naïve adults with attention-deficit hyperactivity disorder

Hsiang-Yuan Lin, MD[1,2+], Luca Cocchi, PhD[2+], Andrew Zalesky, PhD[3], Jinglei Lv, PhD[2], Alistair Perry, PhD[2], Wen-Yih Isaac Tseng, MD, PhD[4,5], Prantik Kundu, PhD[6], Michael Breakspear, MBBS, PhD, FRANZCP[2,7], Susan Shur-Fen Gau, MD, PhD[1,5*]

[1] Department of Psychiatry, National Taiwan University Hospital, and College of Medicine, Taipei, Taiwan.
[2] Systems Neuroscience Group, QIMR Berghofer Medical Research Institute, Brisbane, Queensland, Australia.
[3] Melbourne Neuropsychiatry Centre, The University of Melbourne, Melbourne, Victoria, Australia.
[4] Institute of Medical Device and Imaging, National Taiwan University College of Medicine, Taipei, Taiwan.
[5] Graduate Institute of Brain and Mind Sciences, National Taiwan University College of Medicine, Taipei, Taiwan.
[6] Departments of Radiology and Psychiatry, Icahn School of Medicine at Mount Sinai, New York, NY, USA.
[7] Metro North Mental Health Service, The Royal Brisbane and Women's Hospital, Brisbane, Queensland, Australia.

+ Equally contributed as co-first authors

*Corresponding author:

Susan Shur-Fen Gau

Department of Psychiatry, National Taiwan University Hospital and College of Medicine

No. 7, Chung-Shan South Road, Taipei, Taiwan 10002.

Tel: +886-2-23123456 ext.66802, Fax: +886-2-23812408

Email: gaushufe@ntu.edu.tw

Abstract

Background: Childhood-onset attention-deficit hyperactivity disorder (ADHD) in adults is clinically heterogeneous and commonly presents with different patterns of cognitive deficits. It is unclear if this clinical heterogeneity expresses a dimensional or categorical difference in ADHD. **Methods:** We first studied differences in functional connectivity in multi-echo resting-state functional magnetic resonance imaging (rs-fMRI) acquired from 80 medication-naïve adults with ADHD and 123 matched healthy controls. We then used canonical correlation analysis (CCA) to identify latent relationships between behavioral symptoms and patterns of altered functional connectivity (dimensional biotype) in patients. Clustering methods were implemented to test if the individual associations between resting-state brain connectivity and behavior reflected a non-overlapping categorical biotype. **Results:** Adults with ADHD showed stronger functional connectivity compared to healthy controls, predominantly between the default-mode, cingulo-opercular and subcortical networks. CCA identified a single mode of brain-behavior co-variation, corresponding to an ADHD dimensional biotype. This dimensional biotype is characterized by a unique combination of altered connectivity correlating with symptoms of hyperactivity-impulsivity, inattention, and intelligence. Clustering analyses did not support the existence of distinct categorical biotypes of adult ADHD. **Conclusions:** Overall, our data advance a novel finding that the reduced functional segregation between default-mode and cognitive control networks supports a clinically important dimensional biotype of childhood-onset adult ADHD. Despite the heterogeneity of its presentation, our work suggests that childhood-onset adult ADHD is a single disorder characterized by dimensional brain-behavior mediators.

Introduction

Attention-deficit hyperactivity disorder (ADHD) is a childhood-onset neurodevelopmental disorder whose persistence into adulthood has been increasingly acknowledged (Asherson *et al.*, 2016). ADHD in both children and adults manifests as a heterogeneous condition with significantly varied intensity and types of inattention and hyperactivity-impulsivity symptoms across individuals (Asherson *et al.*, 2016). Individuals with ADHD also commonly present with general cognitive deficits (Fair *et al.*, 2012, Mostert *et al.*, 2015) interacting with clinical symptoms (Cheung *et al.*, 2015, Rommelse *et al.*, 2016).

Although the aetiological markers of ADHD remain elusive, the disorder is associated with functional alterations in whole-brain resting-state networks (Gallo and Posner, 2016). ADHD symptoms, in both adults and children, have consistently been linked to abnormal functional connectivity within and between the default-mode network (DMN), task-positive networks (TPNs, including executive control and attention networks), and mesocorticolimbic circuits (Castellanos and Aoki, 2016, Cocchi *et al.*, 2012a, Lin and Gau, 2015). In line with the clinical expression of ADHD, these networks are widely-known to provide crucial support to higher-order cognitive functions (Cole *et al.*, 2016) and general intelligence (Hearne *et al.*, 2016).

Altered resting-state connectivity has been used to parse clinically heterogeneous children with ADHD into more coherent subgroups (Costa Dias *et al.*, 2015, Gates *et al.*, 2014). However, attempts to stratify ADHD based on resting-state connectivity have so far provided inconsistent results with important caveats from a clinical perspective. For example, connectivity-based clusters have not converged on symptomatically similar subgroups of ADHD across studies (Gates *et al.*, 2014). Previous studies have also isolated subgroups by pooling ADHD and

typically developing controls together, precluding a distinct assessment of possible categories specific to ADHD (Costa Dias *et al.*, 2015, Gates *et al.*, 2014, Marquand *et al.*, 2016). On the other hand, dimensional models of ADHD psychopathology based on behavioral measures are increasingly supported (Marcus and Barry, 2011, Willcutt *et al.*, 2012). Nevertheless, the link between existing dimensional models and brain function remains elusive, with very limited data in the adult population (Asherson *et al.*, 2016, Gallo and Posner, 2016).

Recent advances in neuroimaging methods provide new opportunities to test the dimensional and categorical models of ADHD by using multivariate analyses (e.g., canonical correlation analysis, CCA) of brain-behavior relationships (Drysdale *et al.*, 2017, Smith *et al.*, 2015). Leveraging these new methodological developments, the heterogeneity between individuals with ADHD can be addressed by borrowing and extending the construct of biotype. Here, a biotype delineates a subgroup of individuals with ADHD sharing common behavioral patterns and abnormal resting-state connectivity. A dimensional biotype is defined by abnormal brain-behavior patterns that vary in severity across individuals on a continuum. Conversely, a categorical biotype defines a discrete subgroup of individuals sharing a combined pattern of altered functional connectivity and clinical-cognitive features that are unique and segregated from other individuals. Breaking down ADHD heterogeneity into dimensional or categorical biotypes is important because it will enable the development of targeted research and clinical interventions.

In this study, we assessed complex relationships between clinical and cognitive presentations and abnormal resting-state connectivity in a large medication-naïve sample of adults with ADHD. The principal aim of our analysis was to uncover the existence of dimensional or/and categorical biotypes of childhood-onset adult ADHD. Specifically, we

investigated biotypes that distinguished symptoms of inattention, hyperactivity-impulsivity, and general cognitive functioning (Wechsler, 1997). To maximize the translational value of our work (Drysdale *et al.*, 2017), we focused on a subset of behavioral measures which capture the majority of variance in ADHD phenomenology (Asherson *et al.*, 2016) and are commonly acquired in clinical settings.

Methods

Participants and procedure

The study included 80 medication-naïve adults with childhood-onset ADHD aged 18-39 years, who fulfilled *DSM-IV-TR* criteria for ADHD, and 123 healthy controls with no clinically significant psychopathology. Compared to existing multi-sites studies (Hoogman *et al.*, 2017), we recruited a homogeneous sample that is free from medication and multi-site confounds (e.g., different MR scanners and protocols). The detection of biotypes in our unique sample is also facilitated because the variance in the data cannot be linked to heterogeneous developmental delays and psychiatric comorbidity (Schnack and Kahn, 2016). From a methodological viewpoint, our analyses were tailored so that meaningful ADHD biotypes could be detected with the given sample size (see Supplementary Methods).

The participants were recruited and assessed from the adult ADHD special clinic of the Department of Psychiatry, National Taiwan University Hospital (NTUH), Taipei, Taiwan from March 2014 to December 2016. All participants were recruited via advertizement at the colleges, and websites. The adults interested in the study were first telephone-screened using Chinese version of the Adult ADHD Self-Report Scale v1.1 (Yeh *et al.*, 2008). Those identified as probable cases of ADHD by telephone interview were excluded from the study if

they had ever received psychotropic treatment before. All of other participants were then clinically assessed and diagnosed by a board-certified child psychiatrist (SS Gau) for the presence or absence of ADHD and any other psychiatric disorders. The ADHD diagnosis was further confirmed with the Conners' Adult ADHD Diagnostic Interview (Conners *et al.*, 1999) for current ADHD, and the modified adult version of the ADHD supplement of the Chinese version of the Kiddie-Schedule for Affective Disorders and Schizophrenia–Epidemiological Version (K-SADS-E) for childhood and current ADHD (see Supplementary Information) (Lin and Gau, 2015). Age-matched healthy adult controls without any lifetime diagnosis of ADHD received the same clinical assessments as the ADHD group. Exclusion criteria for all participants included: Any prior systemic medical illness; a history of affective disorders, psychosis, substance use disorder, autism spectrum disorder; current depressive/anxiety symptoms or suicidal ideation; a history of psychotropic treatment, including medication for ADHD; and a full IQ (FIQ) <80, as assessed by Wechsler Adult Intelligence Scale-3rd Edition (Wechsler, 1997). Of the ADHD participants, 47, 32, and one were diagnosed with the DSM-IV inattentive, combined, and hyperactivity-impulsive subtypes, respectively (Table 1 and Supplementary Table 1). Notably, only 61 adults retained the same subtypes across current and childhood presentations (the childhood subtypes were ascertained using the K-SADS-E).

All study procedures were approved by the Research Ethics Committee of the NTUH (201401024RINC; ClinicalTrials.gov number, NCT02642068). All participants provided written informed consent.

Table 1. Demographic and clinical features of the participants

Mean (SD)	**Control (N=123)**	**ADHD (N=80)**	**Statistics**
Age (18-39 years)	25.71 (4.87)	26.73 (5.63)	p=0.171
Sex (M/F)	79/44	56/24	p=0.394
Handedness (R/L)	118/5	63/16	p<0.001
FIQ	109.07 (9.08) (range: 89-138)	106.55 (9.81) (range: 80-137)	p=0.063
VIQ	109.49 (10.18)	107.18 (12.74)	p=0.154
PIQ	110.57 (11.04)	107.53 (15.21)	p=0.101
ADHD symptoms			
Inattention[a]	6.49 (4.84)	19.65 (5.02)	p<0.001
Hyperactivity/Impulsivity[a]	3.12 (4.29)	13.55 (6.52)	p<0.001
Opposition-defiance[a]	3.64 (11.40)	4.16 (5.86)	p<0.001
ASRS-A	13.21 (5.14)	27.08 (4.75)	p<0.001
ASRS-B	8.93 (5.03)	19.94 (6.21)	p<0.001
Mean frame-wise displacement[b] (mm)	0.045 (0.020) (range: 0.014-0.123)	0.049 (0.025) (range: 0.017-0.108)	p=0.233

[a] Measured by the Swanson, Nolan, and Pelham, version IV (SNAP-IV) scale.

[b] Estimated by the Euclidian norm (enorm: square root of the sum of squares of the differences in motion derivatives), computed with AFNI's 1d_tool.py.

Abbreviation: ADHD=attention-deficit hyperactivity disorder; FIQ=full intelligence quotient; PIQ=performance intelligence quotient; VIQ=verbal intelligence quotient; ASRS=Adult ADHD Self-Report Scale; M=male; F=female; R=right; L=left; SD=standard deviation.

Imaging protocols and preprocessing

Neuroimaging data were acquired with a Siemens 3T Tim Trio scanner using a 32-channel head coil at Advanced Biomedical Imaging Lab of the NTUH. All participants completed a standardized resting-state functional magnetic resonance imaging (rs-fMRI) scan.

These fMRI data were acquired using a state-of-the-art multi-echo planar imaging (EPI)

sequence (repetition time=2550 ms; echo time=12, 28, 44 and 60 ms). These data permit unique denoising and analyses using multi-echo independent components analysis (ME-ICA v3.0 beta1; www.bitbucket.org/prantikk/me-ica) (Kundu *et al.*, 2012). In comparison to standard single-echo imaging, this approach enhances the signal-to-noise ratio and addresses concerns regarding non-neural confounding factors in fMRI acquisitions, particularly head motion (Kundu *et al.*, 2017). Preprocessing was carried out using AFNI v16.1.10 and Python v2.7.11 toolkits. Each individual's denoised EPI was co-registered to their T1 image and then non-linearly normalized to the Montreal Neurological Institute template (3-mm isotropic voxel size). The time course was temporally band-pass filtered (0.01~0.1 Hz). *Post-hoc* analysis showed that levels of framewise displacement (computed using AFNI's 1d_tool.py) were similar between ADHD and controls (p=0.233, Table 1). No participants exhibited extreme levels of head motion (translation and rotation rigid-body realignment estimates were <1.5mm and <1.5°). MRI data acquisition and the ME-ICA are detailed in Supplementary Methods.

Whole-brain patterns of altered functional connectivity in ADHD

We delineated ADHD biotypes based on distinct patterns of abnormal resting-state connectivity identified by diagnostic group comparisons (ADHD vs. controls). We reasoned that biologically meaningful ADHD subtypes would be best characterized by a subset of the whole-brain resting-state connectivity features that comprise group differences between ADHD and controls. A graphic representation of the analysis pipeline is presented in Fig. 1.

We generated a whole-brain correlation matrix for each participant, based on a well-validated functional brain parcellation (Power *et al.*, 2011). Eleven of the originally published 264 nodes, mostly the inferior temporal areas, were excluded from analysis owing to incomplete MRI coverage. We additionally included the bilateral nucleus accumbens, which is

implicated in ADHD pathology (Costa Dias *et al.*, 2015). The final parcellation included 255 functional nodes (10-mm-diameter spheres). fMRI time series were extracted from each node by averaging over the representative voxels. The Fisher z-transformation was applied to each correlation coefficient within the matrix.

We employed network-based statistic (NBS) (Zalesky *et al.*, 2010), a validated non-parametric algorithm that controls for multiple comparisons (between all possible edges). NBS was performed on connectivity matrices to identify bivariate patterns of connectivity that differentiated ADHD from healthy controls. NBS is based on the principles underpinning traditional cluster-based thresholding of statistical parametric maps and hence proceeds with a preliminary height threshold (pair-wise connections) followed by a familywise error (FWE)-corrected cluster threshold (topological subnetworks of connections). We used a t-statistic (absolute value) of 3.5 as our initial height threshold (corresponding to $p<0.0005$, two-tailed), followed by a conservative FWE corrected $p<0.05$ for our pair-wise contrasts. This height threshold was identical to the one adopted in our previous neuroimaging investigation in adult ADHD (Cocchi *et al.*, 2012a). The inference was performed using permutation testing (10,000 permutations).

To ensure our results are not specific to any particular parcellation template, we repeated the analysis with functional networks constructed using parcellation templates of different resolution and nature (Supplementary Fig. 1). To further test the robustness of our NBS results, we undertook a confirmatory analysis using data-driven group ICA and functional network connectivity (Jafri *et al.*, 2008) (see Fig. 1 and Supplementary Information).

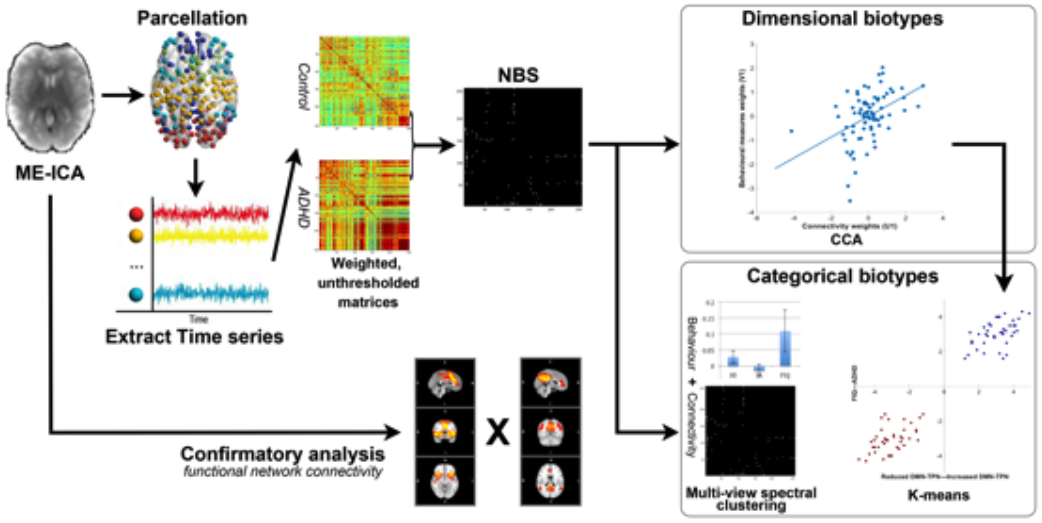

Figure 1. *Overview of data processing and analysis pipeline.* Multi-echo independent component analysis (ME-ICA) was used to denoise eye-closed resting-state imaging data. Functional connectivity matrices were calculated by extracting the average signal time series from validated brain parcellations. The network-based statistic (NBS) was used to assess differences in whole-brain connectivity between 80 drug-naive individuals with ADHD and 123 matched healthy controls. Results from the NBS were corroborated by a data-driven functional network connectivity analysis. Following data reduction steps (see text) functional connectivity and behavioral data were used to perform a canonical correlation analysis (CCA). This analysis allowed to identify hidden relations between resting-state functional connectivity and behavior. The CCA assigns a weight for each functional connection and each symptom such that the level of linear correlation between connectivity and behavioral data across individuals with ADHD is maximized. Permutation testing determined a family-wise error (FWE) corrected p-value for this multivariate correlation (i.e., dimensional biotype). Regarding the discovery of categorical biotype, two complementary approaches were employed: a. *k*-means clustering was used to test if the individual associations between connectivity and behavior form distinct clusters; b. multi-view spectral clustering (Kumar and Daumé, 2011) was implemented using features from symptoms and connectivity (NBS results).

CCA and clustering

CCA is a multivariate statistical method to identify latent, linear relations between combinations of independent and dependent variables (Krzanowski, 2000). The first mode represents canonical correlations corresponding to the maximum co-variation between the two sets of variables. Subsequent modes represent maximum residual, orthogonal co-variation. We implemented CCA to identify modes which relate sets of resting-state connectivity patterns to symptom and cognitive measures of ADHD pathology, within the ADHD cohort. Connections composing the altered resting-state network as identified by the NBS were selected as connectivity features within the CCA. Three behavioral measures were included in the CCA:

factor scores of inattentive and hyperactivity-impulsivity symptoms, and FIQ. As general cognitive functions may modify the clinical presentation of ADHD (Rommelse *et al.*, 2016), moderate its prognosis (Cheung *et al.*, 2015) and influence its clinical heterogeneity (Fair *et al.*, 2012, Mostert *et al.*, 2015), we included FIQ alongside the two main symptoms dimensions of ADHD as the CCA behavioral measures. FIQ is advantageous because it represents a parsimonious account of general cognitive functions, and is easily accessible in clinical routines, which was not the case for cognitive measures adopted in earlier attempts of clustering ADHD (Marquand *et al.*, 2016). Statistical significance was estimated via 100,000 permutations of the rows of one matrix relative to the other. Technical details regarding the CCA are provided in Supplementary Methods.

To test the existence of ADHD categorical biotypes, we implemented complementary analysis strategies using the features derived from CCA modes and combined features from connectivity and clinical symptoms. To assess whether the brain-behavior associations identified by the CCA were evenly distributed or clustered in distinct subgroups, we first employed *k*-means clustering on those linearly projected two-dimensional features by the CCA. To further test the existence of categorical biotypes, we explored joint clustering of connectivity features and behavior features using multi-view spectral clustering. This clustering algorithm maximizes the agreement across clusters identified in different feature spaces (connectivity and behavior) (Kumar and Daumé, 2011). The existence of valid discrete clusters detected using the *k*-means method was determined using state-of-the-art robustness measures including average silhouette width values and the Jaccard similarity (Hennig *et al.*, 2015). For the multi-view spectral clustering, we considered the convergence of the number of clusters yielded across different similarity thresholds. While there are no clear indications

regarding the minimum sample size necessary for clustering analyses, broadly accepted guides (Hennig *et al.*, 2015) argue that our sample size (N=80) is substantially larger than that required to identify clusters using the number of features we employed. Methodological details regarding clustering algorithms are described in the Supplementary Methods.

Results

Altered whole-brain resting-state connectivity in medication-naive adults with ADHD

The application of NBS identified one significant brain network that differentiated adults with ADHD from healthy controls (FWE-corrected p=0.037; Fig. 2 and Supplementary Table 2&3 for details). The ADHD cohort showed stronger resting-state connectivity in this network compared to controls, with increased correlations between the DMN and the TPNs, the DMN and subcortical regions, the salience/cingulo-opercular network and sensory-motor and visual network, as well as the salience/cingulo-opercular network and other TPNs (i.e., dorsal attention and frontoparietal networks) (Fig. 2). Confirmatory analyses using different brain parcellations yielded similar results (Supplementary Fig. 1). Moreover, the main results were replicated using an alternative approach to characterize functional brain networks, using maps derived from ICA decomposition of the data rather than a predefined parcellation (Jafri *et al.*, 2008). Specifically, results from this additional analysis confirmed that ADHD had stronger connectivity between the DMN and the cingulo-opercular/salience/ventral attention networks compared to the controls (false discovery rate corrected q=0.044; Supplementary Fig. 3).

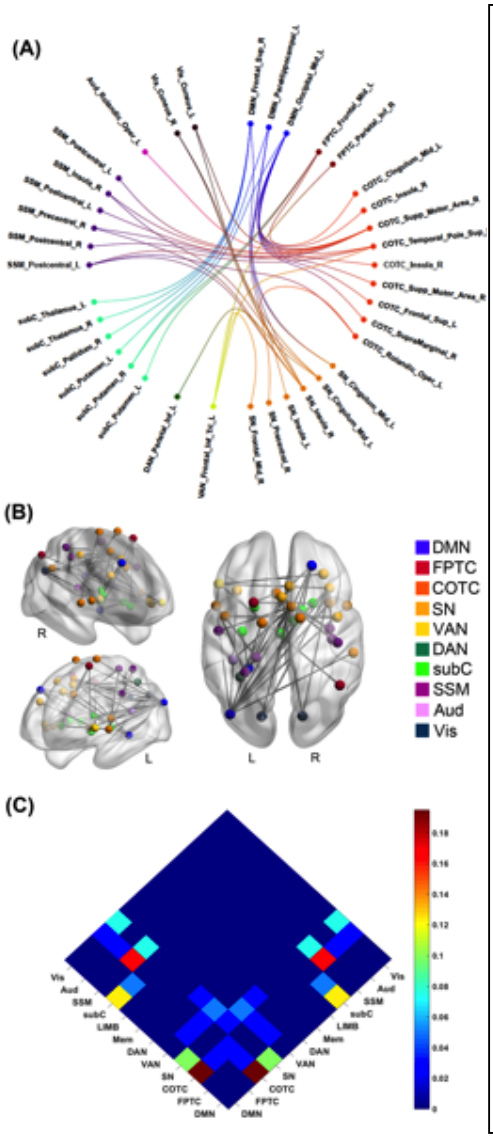

Figure 2. *Group differences in inter-regional functional connectivity*. The network-based statistic (NBS) identified a single network differentiating adult ADHD from healthy controls. This network was hyper-connected (i.e., higher positive correlations) in ADHD compared to controls. Functional brain networks were designated according to Power and colleagues (Power *et al.*, 2011). (A) Circular layout of the network distribution. Colors are used to define different brain networks. (B) Topological representation of brain network hyper-connectivity in ADHD compared to healthy controls. (C) The proportion of functional connections affected by ADHD. The number of connections involving each network pair was normalized by a total number of altered pair-wise connections. Adults with ADHD showed the highest positive functional connectivity between (i) the default mode (DMN) and the salience (SN) networks; (ii) the frontoparietal task control network (FPTC) and subcortical (subC) networks. Network nodes and edges (connections) were visualized using BrainNet Viewer (http://www.nitrc.org/projects/bnv/). Circular layouts were generalized with NeuroMArVL (http://immersive.erc.monash.edu.au/neuromarvl/). Networks/modules were assigned based on the community information provided by Power *et al.* (2011). The anatomical location was identified by the Automatic Anatomical Labeling atlas (http://www.gin.cnrs.fr/en/tools/aal-aal2/) and visual inspection. COTC=cingulo-opercular network; VAN=ventral attention network; DAN=dorsal attention network; SSM=somatosensorimotor network; Aud=auditory network; Vis=visual network; Supp=supplementary; R=right; L=left; Sup=superior; Inf=inferior; Mid=middle; Oper=opercular.

ADHD biotyping

Dimensional biotype

The application of CCA identified one significant mode (r=0.435, FWE-corrected p=0.031) of interdependences between functional connectivity patterns and the behavioral indices of hyperactivity-impulsivity, inattention, and general cognitive functioning (FIQ) (Supplementary Table 4a). Specifically, ADHD adults with high symptoms of hyperactivity and impulsivity showed higher resting-state connectivity in a network comprising the strongest increases in positive connectivity in ADHD compared to controls (Fig. 3A). Symptoms of inattention were

only mildly positively associated with ADHD hyper-connectivity. On the other hand, general cognitive functions, as indexed by IQ scores, were inversely correlated with greater resting-state connectivity (Fig. 3A). The functional connections expressing the strongest positive associations in this mode (mean r=0.68, standard deviation=0.07) involved mainly altered DMN-cingulo-opercular and DMN-subcortical connectivity (Fig. 3B&C and Supplementary Table 5).

Categorical biotype

Results of clustering methods failed to show the existence of a non-overlapping ADHD categorical biotype. Specifically, the application of *k*-means clustering analysis to the CCA weighted behavioral and connectivity values favored a dimensional solution over a categorical one. In particular, the value of the clustering index (average silhouette values) was 0.47 for 2 clusters and 0.48 for 3 clusters (Supplementary Table 6), both below the range considered to support a stable cluster solution. As shown in Supplementary Fig. 4A, ADHD participants were evenly distributed without any clear cluster demarcation. In support of this observation, a multi-view spectral clustering analysis using combined symptom and connectivity features also failed to converge to a stable clustering solution (Supplementary Fig. 4B). The inconsistency in the number of clusters detected across different similarity thresholds indicates that no valid categorical biotypes could be identified for adult ADHD.

Comparison between DSM-IV subtypes and ADHD biotype

There were no significant differences in resting-state connectivity between the combined (N=32) and inattentive (N=47) clinical subtypes (either current or childhood subtypes) using NBS or functional network connectivity.

We also assessed how the DSM-IV-defined ADHD clinical subtypes mapped on the

brain-behavior dimensional axis revealed by our biotyping analysis. As shown in Fig. 3D, participants with different clinical ADHD subtypes were distributed evenly along the one-dimensional axis identified by the CCA.

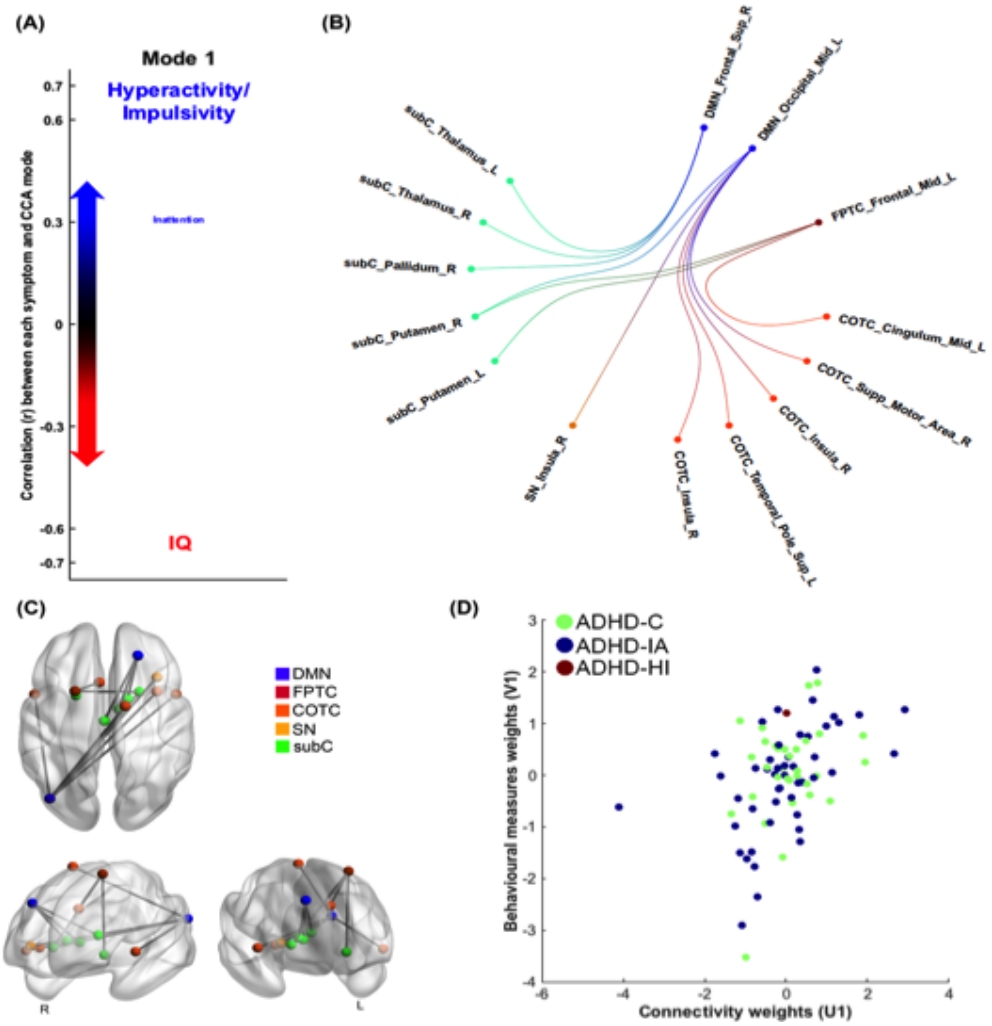

Figure 3. *Canonical correlation analysis (CCA) and ADHD dimensional biotypes*. (A) The CCA analysis identified a single significant (FWE-corrected p=0.031) mode of associations between resting-state connectivity and the behavioral variables of interest. The strength and direction of the variance explained by the CCA mode are indicated in the figure by the vertical position and font size. Adults with ADHD having predominant symptoms of hyperactivity and impulsivity showed higher resting-state connectivity in a network comprising the most (top 25%) hyper-connected edges in ADHD compared to controls (panel B). Conversely, higher cognitive functions (indexed by IQ scores) inversely correlated with (hyper) connectivity in the altered network. Symptoms of inattention were mildly positively associated with resting-state connectivity. (B) Representation of the top 25% node pairs expressed by the CCA mode. (C) This panel represents the circular layout of the top 25% node-pairs. This representation highlights that the majority of hyper-connected edges comprise functional interactions between the default mode (DMN) and the cingulo-opercular network (COTC) and subcortical (subC) networks. (D) Participants with different clinical ADHD subtypes were distributed evenly along the one-dimensional axis identified by the CCA. SN=salience network; FPTC=frontoparietal task control network; R=right; L=left; Sup=superior; Mid=middle; Supp=supplementary.

Discussion

ADHD is characterized by substantial clinical and cognitive heterogeneity. Here, we questioned whether this childhood-onset adult ADHD heterogeneity could be parsed into dimensional or categorical biotypes. Our multivariate analyses showed that inter-individual differences in brain connectivity, clinical symptoms and general cognitive functioning in ADHD define a dimensional biotype (Fig. 3A). We found no evidence for a categorical definition of adult ADHD. Results from this study support the notion of adult ADHD as a single pathological entity, with altered brain-behavior associations varying across a single dimension or spectrum.

Data from our sample allowed the isolation of ADHD biotypes, which are not confounded by developmental delays, general cognitive dysfunction, history of medication use or confounds related to multi-site experiments. Using state-of-the-art multi-echo rs-fMRI data, we showed reduced functional segregation (i.e., higher positive functional connectivity) between the DMN and TPNs in ADHD compared to healthy controls. One of the most robust findings of the fMRI literature in children and adults with ADHD is the increased functional interplay between the DMN and other networks of the brain, especially the cingulo-opercular/salience/ventral attention networks (Castellanos and Aoki, 2016, Gallo and Posner, 2016). In healthy controls, these between-network interactions are known to support dynamic switches between internal and external mental processes (Menon, 2011). Accordingly, studies have shown that the reduced functional segregation between the DMN and other brain networks correlated with attention and hyperactivity symptoms of ADHD (Cocchi *et al.*, 2012a). For example, reduced functional segregation between the DMN and external control networks has been linked to inattention (Barber *et al.*, 2015) and poor inhibitory control (van Rooij *et al.*, 2015) in ADHD youths. Also, the pharmacological enhancement of this between-networks functional segregation improves

ADHD symptoms (Lin and Gau, 2015). The current study extends these previous findings to a larger sample of medication-naïve adults with clinical ADHD. Both NBS and functional network connectivity analyses show increased interactions between DMN and TPNs, supporting the notion that this deficit represents a key brain signature of ADHD (Castellanos and Aoki, 2016). We also identified increased connectivity between salience/cingulo-opercular and all other major brain networks, as well as increased connectivity within the salience/cingulo-opercular network in adults with ADHD. This result supports the notion that altered salience network function significantly impacts the balance between brain systems activity supporting external and internal mental processes (Menon, 2011), and contributes to the emergence of ADHD symptoms (Castellanos and Aoki, 2016).

The CCA showed one significant mode of the population variation that links a pattern of brain connectivity to a specific pattern of covariance between core ADHD symptoms and general intelligence. This analysis suggests that the heterogeneity of ADHD symptomatology can be described by a dimensional biotype. Symptoms of hyperactivity-impulsivity and inattention loaded onto positive associations with connectivity patterns in this mode, whereas IQ loaded onto negative associations. This result indicates that preserved cognitive function acts as a protecting factor for ADHD symptoms in adults (Cheung *et al.*, 2015, Rommelse *et al.*, 2016), whereas lower IQ is associated with chronic and persistent symptoms (Cheung *et al.*, 2015, Keyes *et al.*, 2017). The result that hyperactivity-impulsivity and IQ loaded onto opposing ends of the same axis is in line with previous data on adolescence (Keyes *et al.*, 2017) and highlights the presence of this relationship in adulthood. Moreover, the fact that hyperactivity-impulsivity and inattention loaded onto the same CCA axis supports existing work suggesting a mildly positive correlation between these two ADHD symptom dimensions (Willcutt *et al.*, 2012). The

functional connectivity patterns that were most strongly expressed by this mode included connections between DMN and cingulo-opercular and subcortical brain regions, as well as fronto-parietal-subcortical regions. This further supports proposals derived from healthy cohorts that anti-correlated activity between the DMN and cognitive-control networks underpins optimal brain functions and behaviors (Menon, 2011). Together, results from our CCA analysis highlight that a dimensional biotype defined by behavior-connectivity co-variation explains ADHD heterogeneity.

We revisited prior efforts to utilize neuroimaging or behavioral information to assess the existence of distinct subtypes of individuals with ADHD. Existing studies have defined several ADHD subtypes, mostly in the child population, characterized by co-occurring psychiatric symptoms (Acosta *et al.*, 2008), neuropsychological profiles (Fair *et al.*, 2012, Mostert *et al.*, 2015), temperamental features (Karalunas *et al.*, 2014), and functional connectivity patterns (Costa Dias *et al.*, 2015, Gates *et al.*, 2014). However, these studies have failed to provide a consistent non-overlapping parcellation of ADHD. Herein, we attempted to identify categorical ADHD biotypes by combining resting-state functional connectivity and behavioral data in the largest sample of childhood-onset ADHD to date, but found no evidence for categorical biotypes. In keeping with the inconclusive results of previous attempts, our work highlights the difficulty in parsing the clinical heterogeneity of ADHD into non-overlapping categories. Whereas it could be argued that our clinically homogenous sample may have precluded the identification of categorical biotypes, the distribution of the current sample is consistent with demographic features of adults with childhood-onset ADHD (Asherson *et al.*, 2016). Likewise, our sample allowed the identification of ADHD-specific brain alterations and biotypes. Future studies may build upon the present results to interrogate the impact of factors such as comorbidity,

developmental differences, and medication on the definition of ADHD biotypes. These multi-site endeavors will necessarily require significantly larger samples compared to the present work (Schnack and Kahn, 2016).

Intriguingly, we did not identify functional connectivity differences between the DSM-IV subtypes. Moreover, individuals across both clinically defined ADHD subtypes (i.e., combined and inattentive) were distributed evenly along the axis identified by the CCA, highlighting the challenges of clustering ADHD in non-overlapping subgroups (Marquand *et al.*, 2016). Whether our findings could be generalized to recently-identified late-onset ADHD (Faraone and Biederman, 2016) or children and adolescents with ADHD awaits further testing.

In the current study, we acquired multi-echo rs-fMRI, which allows direct measurement of T2* relaxation rates to facilitate the disambiguation of brain signals from noise and artifacts based on their different echo time dependence (Kundu *et al.*, 2012). The adopted analysis pipeline (see Supplementary Methods) has proven effective in denoising fMRI signal from motion and physiological artifacts in task and rest conditions (Kundu *et al.*, 2017). Despite advantages of our approach in detecting neural signals, we acknowledge the trade-off in acquiring multi-echo data by sacrificing some levels of spatial and temporal resolutions. Future studies are required to assess if dynamic functional connectivity could provide new insights into the link between brain and behavior in ADHD. Finally, it is also important to note that, due to its correlational nature, the CCA is limited in causally linking brain-behavior relationships.

In summary, we here provide the first biotyping of medication-naïve adults with ADHD using neuroimaging and behavioral data. Results showed that patterns of co-variation between resting-state functional connectivity and clinically tractable behavioral measures define a dimensional biotype. Despite the heterogeneity of its clinical presentation, the present work

supports the notion of childhood-onset adult ADHD as a unitary disorder. Specifically, our findings highlight the need to consider its dimensional mediators in research and clinical interventions. This view is endorsed by a recent genome-wide association meta-analysis (Demontis *et al.*, 2017). As a whole, our findings support the importance of mapping the link between brain-behavioral phenotypes and clinical diagnosis, echoing the Research Domain Criteria framework to revise clinically defined constructs using a neurobiologically informed dimensional approach (Cuthbert, 2015).

Acknowledgments

This work was supported by the Ministry of Technology and Science, Taiwan (MOST103-2314-B-002-021-MY3), the National Health Research Institutes, Taiwan (NHRI-EX103-10008PI), and National Taiwan University Hospital (NTUH103-S2458, NTUH104-S2761). The overseas fellowship of H.-Y.L. is supported by the Ministry of Technology and Science, Taiwan (106-2918-I-002-019), and the National Taiwan University Hospital, Taipei, Taiwan. L.C. is supported by the Australian National Health Medical Research Council (L.C., APP1099082).

Declaration of Interest

The authors declare no relevant conflict of interest.

Ethical Standards

The authors assert that all procedures contributing to this work comply with the ethical standards of the relevant national and institutional committees on human experimentation and with the Helsinki Declaration of 1975, as revised in 2008.

References

Abdi, H. & Williams, L. J. (2010). Principal component analysis. **2**, 433-459.

Acosta, M. T., Castellanos, F. X., Bolton, K. L., Balog, J. Z., Eagen, P., Nee, L., Jones, J., Palacio, L., Sarampote, C., Russell, H. F., Berg, K., Arcos-Burgos, M. & Muenke, M. (2008). Latent class subtyping of attention-deficit/hyperactivity disorder and comorbid conditions. **47**, 797-807.

Asherson, P., Buitelaar, J., Faraone, S. V. & Rohde, L. A. (2016). Adult attention-deficit hyperactivity disorder: key conceptual issues. **3**, 568-578.

Barber, A. D., Jacobson, L. A., Wexler, J. L., Nebel, M. B., Caffo, B. S., Pekar, J. J. & Mostofsky, S. H. (2015). Connectivity supporting attention in children with attention deficit hyperactivity disorder. **7**, 68-81.

Beckmann, C. F. & Smith, S. M. (2004). Probabilistic independent component analysis for functional magnetic resonance imaging. **23**, 137-152.

Benjamini, Y. & Hochberg, Y. (1995). Controlling the false discovery rate: a practical and powerful approach to multiple testing. 289-300.

Birn, R. M., Molloy, E. K., Patriat, R., Parker, T., Meier, T. B., Kirk, G. R., Nair, V. A., Meyerand, M. E. & Prabhakaran, V. (2013). The effect of scan length on the reliability of resting-state fMRI connectivity estimates. **83**, 550-558.

Castellanos, F. X. & Aoki, Y. (2016). Intrinsic Functional Connectivity in Attention-Deficit/Hyperactivity Disorder: A Science in Development. **1**, 253-261.

Chang, L. R., Chiu, Y. N., Wu, Y. Y. & Gau, S. S. (2013). Father's parenting and father-child relationship among children and adolescents with attention-deficit/hyperactivity disorder. *Comprehensive psychiatry* **54**, 128-140.

Chao, C. Y., Gau, S. S., Mao, W. C., Shyu, J. F., Chen, Y. C. & Yeh, C. B. (2008). Relationship of attention-deficit-hyperactivity disorder symptoms, depressive/anxiety symptoms, and life quality in young men. *Psychiatry and clinical neurosciences* **62**, 421-426.

Chen, H., Li, K., Zhu, D., Jiang, X., Yuan, Y., Lv, P., Zhang, T., Guo, L., Shen, D. & Liu, T. (2013). Inferring group-wise consistent multimodal brain networks via multi-view spectral clustering. **32**, 1576-1586.

Cheung, C. H., Rijdijk, F., McLoughlin, G., Faraone, S. V., Asherson, P. & Kuntsi, J. (2015). Childhood predictors of adolescent and young adult outcome in ADHD. **62**, 92-100.

Cocchi, L., Bramati, I. E., Zalesky, A., Furukawa, E., Fontenelle, L. F., Moll, J., Tripp, G. & Mattos, P. (2012a). Altered functional brain connectivity in a non-clinical sample of young adults with attention-deficit/hyperactivity disorder. **32**, 17753-17761.

Cocchi, L., Harrison, B. J., Pujol, J., Harding, I. H., Fornito, A., Pantelis, C. & Yucel, M. (2012b). Functional alterations of large-scale brain networks related to cognitive control in obsessive-compulsive disorder. **33**, 1089-1106.

Cole, M. W., Ito, T., Bassett, D. S. & Schultz, D. H. (2016). Activity flow over resting-state networks shapes cognitive task activations. **19**, 1718-1726.

Conners, C. K., D., E. & E., S. (1999). *Conners' adult ADHD rating scales (CAARS)*. MHS: New York.

Costa Dias, T. G., Iyer, S. P., Carpenter, S. D., Cary, R. P., Wilson, V. B., Mitchell, S. H., Nigg, J. T. & Fair, D. A. (2015). Characterizing heterogeneity in children with and without ADHD based on reward system connectivity. **11**, 155-174.

Craddock, R. C., James, G. A., Holtzheimer, P. E., 3rd, Hu, X. P. & Mayberg, H. S. (2012). A whole brain fMRI atlas generated via spatially constrained spectral clustering. **33**, 1914-1928.

Cuthbert, B. N. (2015). Research Domain Criteria: toward future psychiatric nosologies. **17**, 89-97.

Demontis, D., Walters, R. K., Martin, J., Mattheisen, M., Als, T. D., Agerbo, E., Belliveau, R., Bybjerg-Grauholm, J., Bækved-Hansen, M. & Cerrato, F. (2017). Discovery Of The First Genome-Wide Significant Risk Loci For ADHD. 145581.

DiStefano, C., Zhu, M. & Mindrila, D. (2009). Understanding and using factor scores: Considerations for the applied researcher. **14**, 1-11.

Dolnicar, S. (2002). A review of unquestioned standards in using cluster analysis for data-driven market segmentation. In *CD Conference Proceedings of the Australian and New Zealand Marketing Academy Conference 2002 (ANZMAC 2002)*: Deakin University, Melbourne.

Dosenbach, N. U., Nardos, B., Cohen, A. L., Fair, D. A., Power, J. D., Church, J. A., Nelson, S. M., Wig, G. S., Vogel, A. C., Lessov-Schlaggar, C. N., Barnes, K. A., Dubis, J. W., Feczko, E., Coalson, R. S., Pruett, J. R., Jr., Barch, D. M., Petersen, S. E. & Schlaggar, B. L. (2010). Prediction of individual brain maturity using fMRI. **329**, 1358-1361.

Drysdale, A. T., Grosenick, L., Downar, J., Dunlop, K., Mansouri, F., Meng, Y., Fetcho, R. N., Zebley, B., Oathes, D. J., Etkin, A., Schatzberg, A. F., Sudheimer, K., Keller, J., Mayberg, H. S., Gunning, F. M., Alexopoulos, G. S., Fox, M. D., Pascual-Leone, A., Voss, H. U., Casey, B. J., Dubin, M. J. & Liston, C. (2017). Resting-state connectivity biomarkers define neurophysiological subtypes of depression. **23**, 28-38.

Fair, D. A., Bathula, D., Nikolas, M. A. & Nigg, J. T. (2012). Distinct neuropsychological

subgroups in typically developing youth inform heterogeneity in children with ADHD. **109**, 6769-6774.

Faraone, S. V. & Biederman, J. (2016). Can Attention-Deficit/Hyperactivity Disorder Onset Occur in Adulthood? *JAMA psychiatry* **73**, 655-656.

Gallo, E. F. & Posner, J. (2016). Moving towards causality in attention-deficit hyperactivity disorder: overview of neural and genetic mechanisms. **3**, 555-567.

Gates, K. M., Molenaar, P. C., Iyer, S. P., Nigg, J. T. & Fair, D. A. (2014). Organizing heterogeneous samples using community detection of GIMME-derived resting state functional networks. **9**, e91322.

Gau, S. F. & Soong, W. T. (1999). Psychiatric comorbidity of adolescents with sleep terrors or sleepwalking: a case-control study. **33**, 734-739.

Gau, S. S., Chong, M. Y., Chen, T. H. & Cheng, A. T. (2005). A 3-year panel study of mental disorders among adolescents in Taiwan. **162**, 1344-1350.

Gau, S. S., Kessler, R. C., Tseng, W. L., Wu, Y. Y., Chiu, Y. N., Yeh, C. B. & Hwu, H. G. (2007). Association between sleep problems and symptoms of attention-deficit/hyperactivity disorder in young adults. *Sleep* **30**, 195-201.

Gau, S. S., Shang, C. Y., Liu, S. K., Lin, C. H., Swanson, J. M., Liu, Y. C. & Tu, C. L. (2008). Psychometric properties of the Chinese version of the Swanson, Nolan, and Pelham, version IV scale - parent form. **17**, 35-44.

Hearne, L. J., Mattingley, J. B. & Cocchi, L. (2016). Functional brain networks related to individual differences in human intelligence at rest. **6**, 32328.

Hennig, C. (2008). Dissolution point and isolation robustness: robustness criteria for general cluster analysis methods. **99**, 1154-1176.

Hennig, C., Meila, M., Murtagh, F. & Rocci, R. (2015). *Handbook of Cluster Analysis*. CRC Press.

Hoogman, M., Bralten, J., Hibar, D. P., Mennes, M., Zwiers, M. P., Schweren, L. S., van Hulzen, K. J., Medland, S. E., Shumskaya, E., Jahanshad, N., Zeeuw, P., Szekely, E., Sudre, G., Wolfers, T., Onnink, A. M., Dammers, J. T., Mostert, J. C., Vives-Gilabert, Y., Kohls, G., Oberwelland, E., Seitz, J., Schulte-Ruther, M., Ambrosino, S., Doyle, A. E., Hovik, M. F., Dramsdahl, M., Tamm, L., van Erp, T. G., Dale, A., Schork, A., Conzelmann, A., Zierhut, K., Baur, R., McCarthy, H., Yoncheva, Y. N., Cubillo, A., Chantiluke, K., Mehta, M. A., Paloyelis, Y., Hohmann, S., Baumeister, S., Bramati, I., Mattos, P., Tovar-Moll, F., Douglas, P., Banaschewski, T., Brandeis, D., Kuntsi, J., Asherson, P., Rubia, K., Kelly, C., Martino, A. D., Milham, M. P., Castellanos, F. X., Frodl, T., Zentis, M., Lesch, K. P., Reif,

A., Pauli, P., Jernigan, T. L., Haavik, J., Plessen, K. J., Lundervold, A. J., Hugdahl, K., Seidman, L. J., Biederman, J., Rommelse, N., Heslenfeld, D. J., Hartman, C. A., Hoekstra, P. J., Oosterlaan, J., Polier, G. V., Konrad, K., Vilarroya, O., Ramos-Quiroga, J. A., Soliva, J. C., Durston, S., Buitelaar, J. K., Faraone, S. V., Shaw, P., Thompson, P. M. & Franke, B. (2017). Subcortical brain volume differences in participants with attention deficit hyperactivity disorder in children and adults: a cross-sectional mega-analysis. **4**, 310-319.

Huettel, S. A., Song, A. W. & McCarthy, G. (2008). *Functional magnetic resonance imaging*. Sinauer Associates: Sunderland.

Hyvarinen, A. (1999). Fast and robust fixed-point algorithms for independent component analysis. **10**, 626-634.

Jafri, M. J., Pearlson, G. D., Stevens, M. & Calhoun, V. D. (2008). A method for functional network connectivity among spatially independent resting-state components in schizophrenia. **39**, 1666-1681.

Karalunas, S. L., Fair, D., Musser, E. D., Aykes, K., Iyer, S. P. & Nigg, J. T. (2014). Subtyping attention-deficit/hyperactivity disorder using temperament dimensions: toward biologically based nosologic criteria. **71**, 1015-1024.

Keyes, K. M., Platt, J., Kaufman, A. S. & McLaughlin, K. A. (2017). Association of Fluid Intelligence and Psychiatric Disorders in a Population-Representative Sample of US Adolescents. **74**, 179-188.

Kononenko, I. & Kukar, M. (2007). *Machine learning and data mining: introduction to principles and algorithms*. Horwood Publishing.

Krzanowski, W. (2000). *Principles of multivariate analysis*. OUP Oxford.

Kumar, A. & Daumé, H. (2011). A co-training approach for multi-view spectral clustering. In *Proceedings of the 28th International Conference on Machine Learning (ICML-11)*, pp. 393-400.

Kundu, P., Brenowitz, N. D., Voon, V., Worbe, Y., Vertes, P. E., Inati, S. J., Saad, Z. S., Bandettini, P. A. & Bullmore, E. T. (2013). Integrated strategy for improving functional connectivity mapping using multiecho fMRI. **110**, 16187-16192.

Kundu, P., Inati, S. J., Evans, J. W., Luh, W. M. & Bandettini, P. A. (2012). Differentiating BOLD and non-BOLD signals in fMRI time series using multi-echo EPI. **60**, 1759-1770.

Kundu, P., Voon, V., Balchandani, P., Lombardo, M. V., Poser, B. A. & Bandettini, P. (2017). Multi-Echo fMRI: A Review of Applications in fMRI Denoising and Analysis of BOLD Signals.

Lin, H. Y. & Gau, S. S. (2015). Atomoxetine Treatment Strengthens an Anti-Correlated

 19, pyv094.

Lombardo, M. V., Auyeung, B., Holt, R. J., Waldman, J., Ruigrok, A. N., Mooney, N., Bullmore, E. T., Baron-Cohen, S. & Kundu, P. (2016). Improving effect size estimation and statistical power with multi-echo fMRI and its impact on understanding the neural systems supporting mentalizing. **142**, 55-66.

Lv, J., Iraji, A., Ge, F., Zhao, S., Hu, X., Zhang, T., Han, J., Guo, L., Kou, Z. & Liu, T. (2016). Temporal Concatenated Sparse Coding of Resting State fMRI Data Reveal Network Interaction Changes in mTBI. In *International Conference on Medical Image Computing and Computer-Assisted Intervention*, pp. 46-54. Springer.

Marcus, D. K. & Barry, T. D. (2011). Does attention-deficit/hyperactivity disorder have a dimensional latent structure? A taxometric analysis. **120**, 427-442.

Marquand, A. F., Wolfers, T., Mennes, M., Buitelaar, J. & Beckmann, C. F. (2016). Beyond Lumping and Splitting: A Review of Computational Approaches for Stratifying Psychiatric Disorders. **1**, 433-447.

Menon, V. (2011). Large-scale brain networks and psychopathology: a unifying triple network model. **15**, 483-506.

Mostert, J. C., Hoogman, M., Onnink, A. M., van Rooij, D., von Rhein, D., van Hulzen, K. J., Dammers, J., Kan, C. C., Buitelaar, J. K., Norris, D. G. & Franke, B. (2015). Similar Subgroups Based on Cognitive Performance Parse Heterogeneity in Adults With ADHD and Healthy Controls.

Ni, H. C., Lin, Y. J., Gau, S. S., Huang, H. C. & Yang, L. K. (2013a). An Open-Label, Randomized Trial of Methylphenidate and Atomoxetine Treatment in Adults With ADHD. *Journal of attention disorders*.

Ni, H. C., Shang, C. Y., Gau, S. S., Lin, Y. J., Huang, H. C. & Yang, L. K. (2013b). A head-to-head randomized clinical trial of methylphenidate and atomoxetine treatment for executive function in adults with attention-deficit hyperactivity disorder. *The international journal of neuropsychopharmacology* **16**, 1959-1973.

Orvaschel, H., Puig-Antich, J., Chambers, W., Tabrizi, M. A. & Johnson, R. (1982). Retrospective assessment of prepubertal major depression with the Kiddie-SADS-e. *Journal of the American Academy of Child Psychiatry* **21**, 392-397.

Power, J. D., Cohen, A. L., Nelson, S. M., Wig, G. S., Barnes, K. A., Church, J. A., Vogel, A. C., Laumann, T. O., Miezin, F. M., Schlaggar, B. L. & Petersen, S. E. (2011). Functional

network organization of the human brain. **72**, 665-678.

Rommelse, N., van der Kruijs, M., Damhuis, J., Hoek, I., Smeets, S., Antshel, K. M., Hoogeveen, L. & Faraone, S. V. (2016). An evidenced-based perspective on the validity of attention-deficit/hyperactivity disorder in the context of high intelligence. **71**, 21-47.

Schnack, H. G. & Kahn, R. S. (2016). Detecting Neuroimaging Biomarkers for Psychiatric Disorders: Sample Size Matters. **7**, 50.

Shi, J. & Malik, J. (2000). Normalized cuts and image segmentation. **22**, 888-905.

Smith, S. M., Fox, P. T., Miller, K. L., Glahn, D. C., Fox, P. M., Mackay, C. E., Filippini, N., Watkins, K. E., Toro, R., Laird, A. R. & Beckmann, C. F. (2009). Correspondence of the brain's functional architecture during activation and rest. **106**, 13040-13045.

Smith, S. M., Hyvarinen, A., Varoquaux, G., Miller, K. L. & Beckmann, C. F. (2014). Group-PCA for very large fMRI datasets. **101**, 738-749.

Smith, S. M., Nichols, T. E., Vidaurre, D., Winkler, A. M., Behrens, T. E., Glasser, M. F., Ugurbil, K., Barch, D. M., Van Essen, D. C. & Miller, K. L. (2015). A positive-negative mode of population covariation links brain connectivity, demographics and behavior. **18**, 1565-1567.

Swanson, J. M., Kraemer, H. C., Hinshaw, S. P., Arnold, L. E., Conners, C. K., Abikoff, H. B., Clevenger, W., Davies, M., Elliott, G. R., Greenhill, L. L., Hechtman, L., Hoza, B., Jensen, P. S., March, J. S., Newcorn, J. H., Owens, E. B., Pelham, W. E., Schiller, E., Severe, J. B., Simpson, S., Vitiello, B., Wells, K., Wigal, T. & Wu, M. (2001). Clinical relevance of the primary findings of the MTA: success rates based on severity of ADHD and ODD symptoms at the end of treatment. *Journal of the American Academy of Child and Adolescent Psychiatry* **40**, 168-179.

Takahashi, M., Goto, T., Takita, Y., Chung, S. K., Wang, Y. & Gau, S. S. (2014). Open-label, dose-titration tolerability study of atomoxetine hydrochloride in Korean, Chinese, and Taiwanese adults with attention-deficit/hyperactivity disorder. *Asia-Pacific psychiatry : official journal of the Pacific Rim College of Psychiatrists* **6**, 62-70.

Tao, H., Hou, C. & Yi, D. (2014). Multiple-view spectral embedded clustering using a co-training approach. In *Computer Engineering and Networking*, pp. 979-987. Springer.

Van Dijk, K. R., Hedden, T., Venkataraman, A., Evans, K. C., Lazar, S. W. & Buckner, R. L. (2010). Intrinsic functional connectivity as a tool for human connectomics: theory, properties, and optimization. **103**, 297-321.

van Rooij, D., Hartman, C. A., Mennes, M., Oosterlaan, J., Franke, B., Rommelse, N., Heslenfeld, D., Faraone, S. V., Buitelaar, J. K. & Hoekstra, P. J. (2015). Altered neural

connectivity during response inhibition in adolescents with attention-deficit/hyperactivity disorder and their unaffected siblings. **7**, 325-335.

Venkataraman, A., Van Dijk, K. R., Buckner, R. L. & Golland, P. (2009). Exploring Functional Connectivity in Fmri Via Clustering. **2009**, 441-444.

Wechsler, D. (1997). *Wechsler Adult Intelligence Scale - Third Edition (WAIS-III).* Psychological Corporation: San Antonio, TX

Willcutt, E. G., Nigg, J. T., Pennington, B. F., Solanto, M. V., Rohde, L. A., Tannock, R., Loo, S. K., Carlson, C. L., McBurnett, K. & Lahey, B. B. (2012). Validity of DSM-IV attention deficit/hyperactivity disorder symptom dimensions and subtypes. **121**, 991-1010.

Yang, H. N., Tai, Y. M., Yang, L. K. & Gau, S. S. (2013). Prediction of childhood ADHD symptoms to quality of life in young adults: adult ADHD and anxiety/depression as mediators. *Research in developmental disabilities* **34**, 3168-3181.

Yeh, C. B., Gau, S. S., Kessler, R. C. & Wu, Y. Y. (2008). Psychometric properties of the Chinese version of the adult ADHD Self-report Scale. **17**, 45-54.

Yeo, B. T., Krienen, F. M., Sepulcre, J., Sabuncu, M. R., Lashkari, D., Hollinshead, M., Roffman, J. L., Smoller, J. W., Zollei, L., Polimeni, J. R., Fischl, B., Liu, H. & Buckner, R. L. (2011). The organization of the human cerebral cortex estimated by intrinsic functional connectivity. **106**, 1125-1165.

Zalesky, A., Fornito, A. & Bullmore, E. T. (2010). Network-based statistic: identifying differences in brain networks. **53**, 1197-1207.

Supplementary Information

Brain-behavior patterns define a dimensional biotype in medication-naïve adults with attention-deficit hyperactivity disorder

Hsiang-Yuan Lin, MD[1,2+], Luca Cocchi, PhD[2+], Andrew Zalesky, PhD[3], Jinglei Lv, PhD[2], Alistair Perry, PhD[2], Wen-Yih Isaac Tseng, MD, PhD[4,5], Prantik Kundu, PhD[6], Michael Breakspear, MBBS, PhD, FRANZCP[2,7], Susan Shur-Fen Gau, MD, PhD[1,5]*

1. Supplementary Methods

1.1. Data

1.1.1. Measures for ADHD symptoms

1.1.1.1. The Adult Self-Report Scales

The Adult Self-Report Scales (ASRS), an 18-question scale, was developed in conjunction with the revision of the World Health Organization (WHO) Composite International Diagnostic Interview (CIDI). The ASRS consists of two subscales, Inattention (nine items) and Hyperactivity-Impulsivity (nine items), according to the 18 *DSM-IV* ADHD symptom criteria. Each item asks how often a symptom occurred during the last 6 months on a 5-point Likert scale: 0=*never*, 1=*rarely*, 2=*sometimes*, 3=*often*, and 4=*very often*. The psychometric properties of the Chinese ASRS have been established in a sample of 4,329 Taiwanese young adults (Yeh *et al.*, 2008). The intraclass correlations (ICCs) for test–retest reliability ranged from 0.80 for the Inattention subscale, 0.82 for the Hyperactivity-Impulsivity subscale, and .85 for the total score. The internal consistency (Cronbach's α) was high for the Inattention subscale (0.87), the Hyperactivity-Impulsivity subscale (0.85), and the total score (0.91). It has been used in studies on adult ADHD and sleep problems, anxiety/depression symptoms, and quality of life in Taiwan (Chao *et al.*, 2008, Gau *et al.*, 2007).

1.1.1.2. The Swanson, Nolan, and Pelham, Version IV Scale (SNAP-IV)-Parent form

The SNAP-IV is a 26-item rating instrument including the core DSM-IV-derived ADHD subscales of IA, HI and OD subscales (items 1-9, 10-18, and 19-26, respectively) (Swanson *et al.*, 2001). Each item is rated on a 4-point Likert scale, 0-3 for "not at all", "just a little", "quite a lot", and "very much" based on and parents' report. The norm and psychometric properties of the Chinese version of SNAP-IV have been well established in Taiwan by Gau and colleagues (Gau *et al.*, 2008). The scale has good test-retest reliability (ICCs 0.59~0.72), high internal consistency (Cronbach's α>0.88) and discriminative validity (Gau *et al.*, 2008) and is commonly used in clinical evaluation and research in Taiwanese child and adolescent

populations (Yang *et al.*, 2013).

1.1.1.3. The modified adult version of the ADHD supplement of the Chinese version of the Schedule for Affective Disorders and Schizophrenia–Epidemiological Version (K-SADS-E)

The K-SADS-E is a semi-structured interview scale for the systematic assessment of both past and current episodes of mental disorders in children and adolescents (Orvaschel *et al.*, 1982). Development of the Chinese K-SADS-E was completed by the Child Psychiatry Research Group in Taiwan (Gau and Soong, 1999). This included a two-stage translation and modification for several items with psycholinguistic equivalents relevant to the Taiwanese culture and further modification to meet the DSM-IV diagnostic criteria, with high reliability (generalized kappa coefficients ranging from 0.73 to 0.96 for all mental disorders) and validity (sensitivity 78% and specificity 98%) (Gau *et al.*, 2005). In order to obtain the information about ADHD symptoms and diagnoses in adulthood according to the DSM-IV diagnostic criteria, semi-structured interviews were conducted using both the modified adult ADHD supplement and the Conners' Adult ADHD Diagnostic Interview for DSM-IV (Takahashi *et al.*, 2014). The results showed that the ADHD diagnosis in childhood and current adulthood based on the two clinical instruments achieved total agreement (i.e., people who had been diagnosed with ADHD in childhood and/or current adulthood using the modified adult ADHD supplement of the K-SADS-E also acquired the ADHD diagnosis based on the the Conners' Adult ADHD Diagnostic Interview).

1.1.2. MRI acquisition parameters

All participants were instructed to remain still with their eyes closed and relax while undergoing a 7 min 39 sec resting-state functional magnetic resonance imaging (rs-fMRI) scan. Wakefulness was checked immediately after the sequence was completed, and all participants denied falling asleep during rs-fMRI scans. The duration of the rs-fMRI sequence was decided to limit the chance of possible fluctuations in participants' wakefulness and in-scanner motion while allowing the acquisition of sufficient blood-oxygen-level-dependent (BOLD) signal (Birn *et al.*, 2013, Van Dijk *et al.*, 2010). Scans were obtained in the order with the localizer and rs-fMRI scans being obtained first. T1-weighted anatomical scans (MPRAGE pulse sequences) and diffusion spectrum imaging, which was not analyzed here, were acquired thereafter. Functional images were acquired with a multi-echo echo-planar imaging sequence with online reconstruction (repetition time=2.55 sec; flip angle=90°; matrix size=64 × 64; in-plane resolution=3.75 mm; FOV=240 mm; 31 oblique slices, alternating slice acquisition slice thickness 3.75 mm with 10% gap; iPAT factor=3; bandwidth=1,698 Hz/pixel; echo

time (TE)=12, 28, 44 and 60 msec). Anatomical images were acquired using a T1-weighted magnetization prepared rapid gradient echo (MPRAGE) sequence (256 × 256 FOV – field of view; 1-mm in-plane resolution; inversion time, 900 msec).

1.2. Analyses

1.2.1. Multi-echo independent component analysis (ME-ICA)

ME-ICA initially decomposed multi-echo rs-fMRI data into independent components using FastICA (Hyvarinen, 1999). Independent components were subsequently categorized as BOLD or non-BOLD components based on Kappa and Rho values, which were yielded from signal models reflecting the BOLD-like or non-BOLD-like signal decay processes (Kundu *et al.*, 2012). BOLD-related signals show linear dependence of percent signal changes on TE, which is the characteristic of the T2* decay (Huettel *et al.*, 2008). On the other hand, non-BOLD signal amplitudes demonstrate TE-independence. TE dependence of BOLD signal was measured using the pseudo-*F*-statistic Kappa, with components that scaled strongly with TE having high Kappa scores. Non-BOLD components were identified by TE independence measured by the pseudo-*F*-statistic Rho. By removing non-BOLD components, data were denoised for head motion, physiological, and scanner artifacts (Kundu *et al.*, 2013). Spatial smoothing was not conducted for the denoised normalized data as per the recommendation by Lombardo and colleagues (Lombardo *et al.*, 2016).

1.2.2. Functional network connectivity analysis

1.2.2.1. Independent Component Analysis (ICA)

After preprocessing, the temporally concatenated probabilistic ICA algorithm (temporally concatenated) implemented in FSL MELODIC (Beckmann and Smith, 2004) was used to analyze the rs-fMRI data of all participants. Non-brain voxels were masked with voxel-wise demeaning of the data and normalization of the voxel-wise variance. Next, the processed data were whitened and projected into a 20-dimensional subspace using a Principal Components Analysis (PCA). This step provided a fine-grained decomposition of interconnected brain regions (Smith *et al.*, 2009). These whitened observations were decomposed into sets of vectors that describe signal variation across (i) the temporal domain (time courses), (ii) the session/subject domain, and (iii) the spatial domain (spatial maps). This decomposition was implemented through a non-Gaussian spatial source distribution using a fixed-point iteration

technique (Hyvarinen, 1999). Estimated component maps were divided by the standard deviation of the residual noise, with a threshold of 0.5 set (the probability that needed to be exceeded by a voxel to be considered 'active' in the component of interest) by fitting a mixture model to the histogram of intensity values (Beckmann and Smith, 2004).

We selected resting-state networks according to their known spatial distribution (Cocchi *et al.*, 2012b, Smith *et al.*, 2009, Yeo *et al.*, 2011). We extracted 20 ICA components, 14 of which are consistently identified as canonical resting-state networks (Yeo *et al.*, 2011). The similarity of these 14 resting-state networks with those previously identified was quantified using spatial correlation (all spatial correlation values >0.4) and confirmed by visual inspection. Only these 14 components (networks) were considered in subsequent analyses (Supplementary Fig. 2A).

1.2.2.2. Functional Network Connectivity

The summary time-course for each resting-state network was calculated at the individual participant's level by spatial regression of the full set of 20 ICA components against each participant's denoised rs-fMRI data. This approach models are overlapping variance to account for the potential effects of residual noise captured by the non-physiological valid components (N=6). We calculated functional network connectivity (FNC) (Jafri *et al.*, 2008, Lv *et al.*, 2016) using the Pearson correlation coefficient between each other summary time course. This resulted in a 3D FNC matrix with the dimensions of 14 × 14 (networks) × 203 (participants). Group differences in FNC were tested for each pair of networks using one-way analysis of variance (ANOVA), and FNC with significant group differences were further tested by 2-sample t-test to determine the direction of the difference. The significance threshold was set at $q<0.05$, corrected for multiple comparisons using false discovery rate (FDR) (Benjamini and Hochberg, 1995).

1.2.3. Principal component analysis for ADHD symptoms

To circumvent reporting biases (Asherson *et al.*, 2016), core ADHD symptoms were encapsulated as factor scores (DiStefano *et al.*, 2009) derived from a principal component analysis (PCA) of self-, parents-, and clinician-reported measures, including self-rated Adult ASRS (Yeh *et al.*, 2008), parent-rated SNAP-IV (Gau *et al.*, 2008), as well as clinician-rated modified adult version of the ADHD supplement of the Chinese version of the K-SADS-E (Chang *et al.*, 2013, Ni *et al.*, 2013a, Ni *et al.*, 2013b) (the number of ADHD measures used in the PCA was 3). Two principal components were extracted, which explained 88.25% of the total

variance. Factors were orthogonalized using Varimax rotation. Among them, the first component explained 51.58% of the total variance, and all of the hyperactivity-impulsivity subscales from the above three measures were consistently loaded on this component. The second component explained 36.67% of the total variance, and scores of inattention subdomain across 3 measures were loaded on the component. The principal component analysis was implemented using IBM SPSS Statistics for Macintosh, Version 22.0 (IBM Corp., Armonk, NY, USA).

Symptoms scores patterns loaded onto two components (rotated component matrix)

	Component	
	1 (Hyperactivity-impulsivity)	2 (Inattention)
SNAP_Inattention	0.244	0.743
SNAP_Hyperactivity-impulsivity	0.842	0.182
K-SADS-E_Inattention	0.224	0.806
K-SADS-E_ Hyperactivity-impulsivity	0.798	0.172
ASRS-A	0.227	0.871
ASRS-B	0.754	0.416

1.2.4. Canonical correlation analysis (CCA)

Both connectivity and behavioral measures were normalized and demeaned. A further regression of in-scanner head motion confounds also performed following the approach of Smith and colleagues (Smith *et al.*, 2015) (http://www.fmrib.ox.ac.uk/analysis/HCP-CCA). To avoid overfitting the CCA, a PCA was undertaken using the FSLNets toolbox (Smith *et al.*, 2014) to reduce the dimensionality of the deconfounded functional connectivity matrix to three eigenvectors (explaining 31.83% of the total variance in the connectivity matrix; Supplementary Fig. 2). The data was reduced to this resolution to keep the methodological steps as per Smith et al. (Smith *et al.*, 2015), given the three behavioral measures selected in the CCA. We note that no consensus exists for component number selection (Abdi and Williams, 2010). Thus, we also employed a confirmatory CCA analysis based on a larger dimensionality of 5 eigenvectors (explaining 43.9% of the variance in the connectivity matrix). The primary (3 eigenvectors, r=0.435, FWE-corrected p=0.031) and confirmatory CCA (r=0.459, FWE-corrected p=0.049; Supplementary Table 4b) yielded similar results. Thus, only results from the primary CCA are reported in the main text.

We next assessed which functional connections were most strongly expressed by

variations in the original sets of connections captured by each CCA mode. CCA provides an output vector describing the extent (weight) to which a given individual's connectivity pattern correlated with the CCA mode. We correlated this vector against the original connectivity matrix identified by the NBS analysis to obtain a vector mapping the relative weights and directional signs of the association between resting-state connectivity and the CCA mode (weighted feature vector). In line with what previously done, the strongest (top 25%) absolute values in this vector were retained to define the strongest associations between individual connectivity weights and behavioral measures (Smith *et al.*, 2015).

1.2.5. Clustering algorithms for categorically subtyping ADHD

To test the existence of ADHD categorical biotypes, we implemented several complementary analyses using the connectivity and clinical features derived from the significant CCA mode, and combined features from connectivity and clinical symptoms, respectively.

1.2.5.1. k-means clustering algorithm based on brain-behavior features derived from the significant CCA mode.

To assess whether the brain-behavior associations identified by the CCA could be clustered into non-overlapping subgroups, we first used *k*-means clustering on the features linearly projected by the CCA. This standard clustering procedure uses individual brain-behavior associations to assign each participant to exactly one of *k* clusters (based on clinical ADHD subtypes, a *k*=2 or 3 was used here) (Venkataraman *et al.*, 2009). To reach stable clustering results, for each setting of *k*, clustering was repeated for 10,000 times so that the participants-to-centroid distances within-cluster sum-of-squares were minimized.

1.2.5.2. Multi-view spectral clustering algorithm based on features of functional connectivity and clinical symptoms

With regards to multi-view spectral clustering algorithm (Kumar and Daumé, 2011, Shi and Malik, 2000), we considered clusters derived from the analysis of altered functional connectivity in ADHD compared to controls and features related to clinical symptoms/IQ as two views contributing to the clustering. Using the multi-view spectral clustering framework, the substantial variability of categorical subgrouping across multimodal features (connectivity and behavior) could be modeled and accounted for. This novel clustering method has the advantage of effectively addressing heterogeneity in the considered features by maximizing the agreement across multimodal clusters (Kumar and Daumé, 2011, Shi and Malik, 2000).

Spectral clustering uses connectivity (*denoised NBS results*) and clinical features (*inattention*, *hyperactivity-impulsivity*, *and IQ*), respectively, to generate two graphs. Nodes

within the graphs represent individuals with ADHD whereas the edges represent the similarities between nodes (individuals). The two graphs (one mapping connectivity and one mapping behavior) were then partitioned using the normalized cut strategy, in which the top *k* eigenvectors of the normalized graph Laplacian, which carries the most discriminative information, are adopted to cut the graphs into clusters efficiently. Subsequent co-training algorithms search for target clusters that predict same labels for co-occurring patterns in each view. The spectral clustering algorithm of bi-partitioning sub-graph stopped when the normalized cut value (representing the similarity between the subjects within each possible cluster) is larger than the pre-set threshold. There is no consensus regarding the optimal threshold to be used. Thus, we examined thresholds ranging from 0.2 to 0.9 (incremental of 0.1) (Chen *et al.*, 2013). We used 10,000 iterations for co-training algorithms to converge on stable clusters (permuting for each threshold).

1.2.5.3. Validity of k-means clustering

We verify the validity of *k*-means clustering using average silhouette width values (Kononenko and Kukar, 2007) and Jaccard similarity (Hennig, 2008). This information is provided in Supplementary Table 5.

The silhouette width value is a combination measure assessing intra-cluster homogeneity and inter-cluster separation. It is calculated by measuring how similar that point is to points in its own cluster when compared to points in other clusters. The cutoffs to interpret the validity of *k*-means clustering based on average silhouette width values are as follows (Kononenko and Kukar, 2007):

0.71-1.0 A strong structure has been found.
0.51-0.70 A reasonable structure has been found.
0.26-0.50 The structure is weak and could be artificial. Try additional methods of data analysis.
<0.25 No substantial structure has been found.

Jaccard's similarity (Hennig, 2008) is defined as the size of the intersection divided by the size of the union of the assigned clusters and the resulting partitions from resampling pipelines. It allows estimating the frequency with which similar clusters were recovered in the data. The clustering results with Jaccard's similarity <0.5 are considered unstable (Hennig, 2008).

1.2.5.4. The issue of sample size for clustering analyses

There are no clear indication regarding the minimum sample size necessary for clustering

analyses. However, it is suggested that the minimal sample size for clustering analyses should not be less than 2^m cases (m=number of features used), with $5*2^m$ considered preferable (Dolnicar, 2002). In the present study, we fed features linearly projected by the CCA (i.e., 1 for the brain connectivity feature; 1 for the behavior feature) into *k*-means clustering. That is, the minimum sample size for *k*-means clustering is 20 subjects (i.e., $5*2^2=20$). Concerning the multi-view spectral clustering, there has been very limited prior work investigating the minimum sample size required to obtain meaningful clusters. The multi-view spectral clustering algorithm is, however, considered robust for the high dimensionality and small-sample-size problem (Tao *et al.*, 2014). Indeed, a smaller sample size is generally required to obtain a solution (i.e., the most robust clustering results) using multi-view spectral clustering compared to single-view clustering (Kumar and Daumé, 2011).

In keeping with the above, the current sample size (N=80 ADHD) is appropriate for both k-means and spectral clustering (Dolnicar, 2002, Kumar and Daumé, 2011, Tao *et al.*, 2014).

2. Supplementary Tables

Supplementary Table 1a. Demographics among attention-deficit hyperactivity subtypes (ADHD) (based on the current presentation of ADHD psychopathology)

Mean (SD)	**ADHD-C (N=32)**	**ADHD-I (N=47)**	**Statistics**
Age	27.54 (5.15)	26.33 (5.89)	*p*=0.352
Sex (M/F)	25/7	30/17	*p*=0.319
Handedness (R/L)	24/8	38/9	*p*=0.800
FIQ	108.03 (8.47)	105.36 (10.61)	*p*=0.238
VIQ	110.00 (11.36)	105.34 (13.51)	*p*=0.113
PIQ	109.88 (9.41)	105.49 (17.90)	*p*=0.208
Mean frame-wise displacement[a] (mm)	0.050 (0.025)	0.048 (0.025)	*p*=0.737

==========

Supplementary Table 1b. Demographics among attention-deficit hyperactivity (ADHD) subtypes (based on the childhood presentation of ADHD psychopathology)

Mean (SD)	**ADHD-C (N=51)**	**ADHD-I (N=28)**	**Statistics**
Age	27.10 (5.85)	26.32 (5.20)	*p*=0.557
Sex (M/F)	16/12	39/12	*p*=0.161
Handedness (R/L)	39/12	24/4	*p*=0.564
FIQ	105.98 (9.43)	107.29 (10.64)	*p*=0.576
VIQ	106.94 (12.37)	107.75 (13.80)	*p*=0.790
PIQ	106.59 (16.63)	108.50 (12.11)	*p*=0.594
Mean frame-wise displacement[a] (mm)	0.049 (0.024)	0.049 (0.026)	*p*=0.917

[a] Estimated by the Euclidian norm (enorm: square root of the sum of squares of the differences in motion derivatives), computed with AFNI's 1d_tool.py.

Abbreviation: -C=combined subtype; -I=inattentive subtype; FIQ=full intelligence quotient; PIQ=performance intelligence quotient; VIQ=verbal intelligence quotient; M=male; F=female; R=right; L=left; SD=standard deviation.

Supplementary Table 2. Details of the nodes within the altered network of ADHD (network-based statistics, NBS)

	MNI coordinates		
Nodes	x	y	z
DMN_Frontal_Sup_R	22	39	39
DMN_Occipital_Mid_L	-41	-75	26
DMN_ParaHippocampal_L	-26	-40	-8
FPTC_Frontal_Mid_L	-23	11	64
FPTC_Parietal_Inf_R	44	-53	47
SN_Precentral_R	42	0	47
SN_Insula_L	-35	20	0
SN_Insula_R	36	22	3
SN_Cingulum_Mid_L	-1	15	44
SN_Frontal_Mid_R	31	33	26
SN_Cingulum_Mid_L	5	23	37
COTC_Frontal_Sup_L	-16	-5	71
COTC_SupraMarginal_R	54	-28	34
COTC_Rolandic_Oper_L	-45	0	9
COTC_Supp_Motor_Area_R	13	-1	70
COTC_Insula_R	49	8	-1
COTC_Temporal_Pole_Sup_L	-51	8	-2
COTC_Supp_Motor_Area_R	7	8	51
COTC_Insula_R	36	10	1
COTC_Cingulum_Mid_L	-5	18	34
SN_Frontal_Mid_R	31	33	26
SN_Cingulum_Mid_L	5	23	37
COTC_Frontal_Sup_L	-16	-5	71
COTC_SupraMarginal_R	54	-28	34
COTC_Rolandic_Oper_L	-45	0	9
COTC_Supp_Motor_Area_R	13	-1	70
COTC_Insula_R	49	8	-1
COTC_Temporal_Pole_Sup_L	-51	8	-2
COTC_Supp_Motor_Area_R	7	8	51

COTC_Insula_R	36	10	1
COTC_Cingulum_Mid_L	-5	18	34
DAN_Parietal_Inf_L	-33	-46	47
VAN_Frontal_Inf_Tri_L	-49	25	-1
subC_Putamen_L	-22	7	-5
subC_Putamen_R	23	10	1
subC_Pallidum_R	15	5	7
subC_Thalamus_R	9	-4	6
subC_Thalamus_L	-2	-13	12
Vis_Cuneus_R	15	-77	31
Vis_Cuneus_L	-16	-77	34

Abbreviations: ADHD=attention-deficit hyperactivity disorder; MNI=Montreal Neurological Institute; DMN=default mode network; SN=salience network; COTC=cingulo-opercular network; FPTC=frontoparietal task control network; VAN=ventral attention network; DAN=dorsal attention network; SSM=somatosensorimotor network; Aud=auditory network; Vis=visual network; subC=subcortical; Supp=supplementary; R=right; L=left; Sup=superior; Inf=inferior; Mid=middle; Oper=opercular.

Supplementary Table 3. Average values of functional connectivity in the pairwise connections of interest (network-based statistics, NBS)

Pairs		Control			ADHD		
Network_Region	**Network_Region**	**Mean**	**STE**	**STD**	**Mean**	**STE**	**STD**
DMN_Occipital_Mid_L	SN_Insula_L	0.211	0.022	0.241	0.339	0.029	0.263
DMN_Occipital_Mid_L	SN_Insula_R	0.118	0.024	0.266	0.298	0.027	0.239
DMN_Frontal_Sup_R	SN_Cingulum_Mid_L	0.249	0.028	0.315	0.420	0.039	0.347
DMN_ParaHippocampal_L	SN_Cingulum_Mid_L	0.108	0.023	0.257	0.249	0.032	0.286
DMN_Occipital_Mid_L	COTC_Frontal_Sup_L	0.238	0.028	0.311	0.420	0.036	0.324
DMN_Occipital_Mid_L	COTC_SupraMarginal_R	0.273	0.023	0.258	0.414	0.031	0.279
SN_Precentral_R	COTC_Rolandic_Oper_L	0.249	0.024	0.266	0.398	0.031	0.280
DMN_Occipital_Mid_L	COTC_Supp_Motor_Area_R	0.114	0.027	0.294	0.278	0.036	0.321
DMN_Occipital_Mid_L	COTC_Insula_R	0.057	0.025	0.279	0.210	0.033	0.293
DMN_Occipital_Mid_L	COTC_Temporal_Pole_Sup_L	0.199	0.026	0.288	0.366	0.037	0.334
DMN_Occipital_Mid_L	COTC_Supp_Motor_Area_R	0.170	0.025	0.276	0.308	0.031	0.275
DMN_ParaHippocampal_L	COTC_Supp_Motor_Area_R	0.156	0.023	0.251	0.284	0.026	0.229
DMN_Occipital_Mid_L	COTC_Insula_R	0.180	0.023	0.253	0.310	0.029	0.255
FPTC_Frontal_Mid_L	COTC_Cingulum_Mid_L	0.472	0.029	0.317	0.630	0.030	0.268
SN_Cingulum_Mid_L	DAN_Parietal_Inf_L	0.332	0.023	0.257	0.494	0.032	0.290
FPTC_Parietal_Inf_R	VAN_Frontal_Inf_Tri_L	0.073	0.025	0.273	0.212	0.029	0.264
SN_Insula_R	VAN_Frontal_Inf_Tri_L	0.129	0.027	0.303	0.283	0.029	0.260
SN_Frontal_Mid_R	VAN_Frontal_Inf_Tri_L	0.062	0.022	0.244	0.193	0.026	0.228
COTC_Temporal_Pole_Sup_L	VAN_Frontal_Inf_Tri_L	0.362	0.028	0.307	0.541	0.032	0.288
FPTC_Frontal_Mid_L	subC_Putamen_L	0.264	0.019	0.209	0.384	0.026	0.234
DMN_Occipital_Mid_L	subC_Putamen_R	0.172	0.020	0.219	0.292	0.026	0.233
FPTC_Frontal_Mid_L	subC_Putamen_R	0.283	0.020	0.219	0.419	0.022	0.199
DMN_ParaHippocampal_L	subC_Putamen_L	0.281	0.020	0.224	0.407	0.028	0.253
DMN_Frontal_Sup_R	subC_Pallidum_R	0.212	0.020	0.221	0.347	0.033	0.291
DMN_Frontal_Sup_R	subC_Thalamus_R	0.210	0.022	0.242	0.364	0.033	0.295
DMN_Frontal_Sup_R	subC_Thalamus_L	0.163	0.024	0.266	0.323	0.033	0.292
SN_Insula_R	SSM_Postcentral_L	0.316	0.021	0.232	0.437	0.027	0.237
COTC_Rolandic_Oper_L	SSM_Postcentral_L	0.451	0.027	0.299	0.596	0.027	0.243
COTC_Temporal_Pole_Sup_L	SSM_Postcentral_L	0.462	0.026	0.290	0.616	0.034	0.305

COTC_Supp_Motor_Area_R	SSM_Postcentral_R	0.295	0.028	0.308	0.449	0.031	0.279
SN_Insula_R	SSM_Precentral_R	0.332	0.024	0.261	0.472	0.026	0.234
COTC_Supp_Motor_Area_R	SSM_Precentral_R	0.364	0.027	0.300	0.537	0.029	0.260
COTC_Temporal_Pole_Sup_L	SSM_Postcentral_L	0.397	0.026	0.284	0.566	0.036	0.326
SN_Cingulum_Mid_L	SSM_Insula_R	0.322	0.024	0.264	0.468	0.033	0.294
COTC_Supp_Motor_Area_R	SSM_Insula_R	0.319	0.025	0.272	0.478	0.032	0.290
COTC_Supp_Motor_Area_R	SSM_Postcentral_L	0.243	0.025	0.272	0.389	0.032	0.286
COTC_Supp_Motor_Area_R	Aud_Rolandic_Oper_L	0.337	0.025	0.279	0.481	0.031	0.280
SN_Insula_R	Vis_Cuneus_R	0.212	0.022	0.247	0.337	0.028	0.251
SN_Cingulum_Mid_L	Vis_Cuneus_R	0.257	0.023	0.255	0.396	0.030	0.267
SN_Insula_R	Vis_Cuneus_L	0.260	0.023	0.257	0.390	0.028	0.249
COTC_Supp_Motor_Area_R	Vis_Cuneus_L	0.268	0.022	0.247	0.409	0.025	0.224

Abbreviations: ADHD=attention-deficit hyperactivity disorder; STE=standard error; STD=standard deviation; DMN=default mode network; SN=salience network; COTC=cingulo-opercular network; FPTC=frontoparietal task control network; VAN=ventral attention network; DAN=dorsal attention network; SSM=somatosensorimotor network; Aud=auditory network; Vis=visual network; subC=subcortical; Supp=supplementary; R=right; L=left; Sup=superior; Inf=inferior; Mid=middle; Oper=opercular.

Supplementary Table 4a. The significant canonical correlation analysis (CCA) mode (p<0.05, family-wise error corrected) of the primary analysis.

CCA mode	One
df_1	9
df_2	180.25
F	2.11
r	0.435
Wilk's lambda	0.7835
Familywise error corrected p	0.0305

==========

Supplementary Table 4b. The significant CCA mode (p<0.05, family-wise error corrected) based on the 5 eigenvectors derived from the connectivity matrix.

CCA mode	One
df_1	15
df_2	199.17
F	1.72
r	0.459
Wilk's lambda	0.7142
Familywise error corrected p	0.0489

Supplementary Table 5. Canonical correlation analysis (CCA) mode connectivity weight and associated interregional pairs

Pairs		**CCA edge strength modulation**
Network_Region	**Network_Region**	
DMN_Occipital_Mid_L	SN_Insula_R	0.617
DMN_Occipital_Mid_L	COTC_Supp_Motor_Area_R	0.686
DMN_Occipital_Mid_L	COTC_Insula_R	0.828
DMN_Occipital_Mid_L	COTC_Temporal_Pole_Sup_L	0.788
DMN_Occipital_Mid_L	COTC_Insula_R	0.689
FPTC_Frontal_Mid_L	COTC_Cingulum_Mid_L	0.616
FPTC_Frontal_Mid_L	subC_Putamen_L	0.618
DMN_Occipital_Mid_L	subC_Putamen_R	0.734
FPTC_Frontal_Mid_L	subC_Putamen_R	0.606
DMN_Frontal_Sup_R	subC_Pallidum_R	0.616
DMN_Frontal_Sup_R	subC_Thalamus_R	0.635
DMN_Frontal_Sup_R	subC_Thalamus_L	0.673

Abbreviations: DMN=default mode network; SN=salience network; COTC=cingulo-opercular network; FPTC=frontoparietal task control network; subC=subcortical; R=right; L=left; Sup=superior; Mid=middle; Supp=supplementary.

Supplementary Table 6. Validity indices of *k*-means clustering method (based on the feature vectors of individual participant's weight derived from the connectivity and symptoms matrices of canonical correlation analysis)

***k*-means clustering**		
	2 clusters	3 clusters
Jaccard similarity	0.3276	0.5667
Average silhouette width values	0.4668	0.4773

3. Supplementary Figures

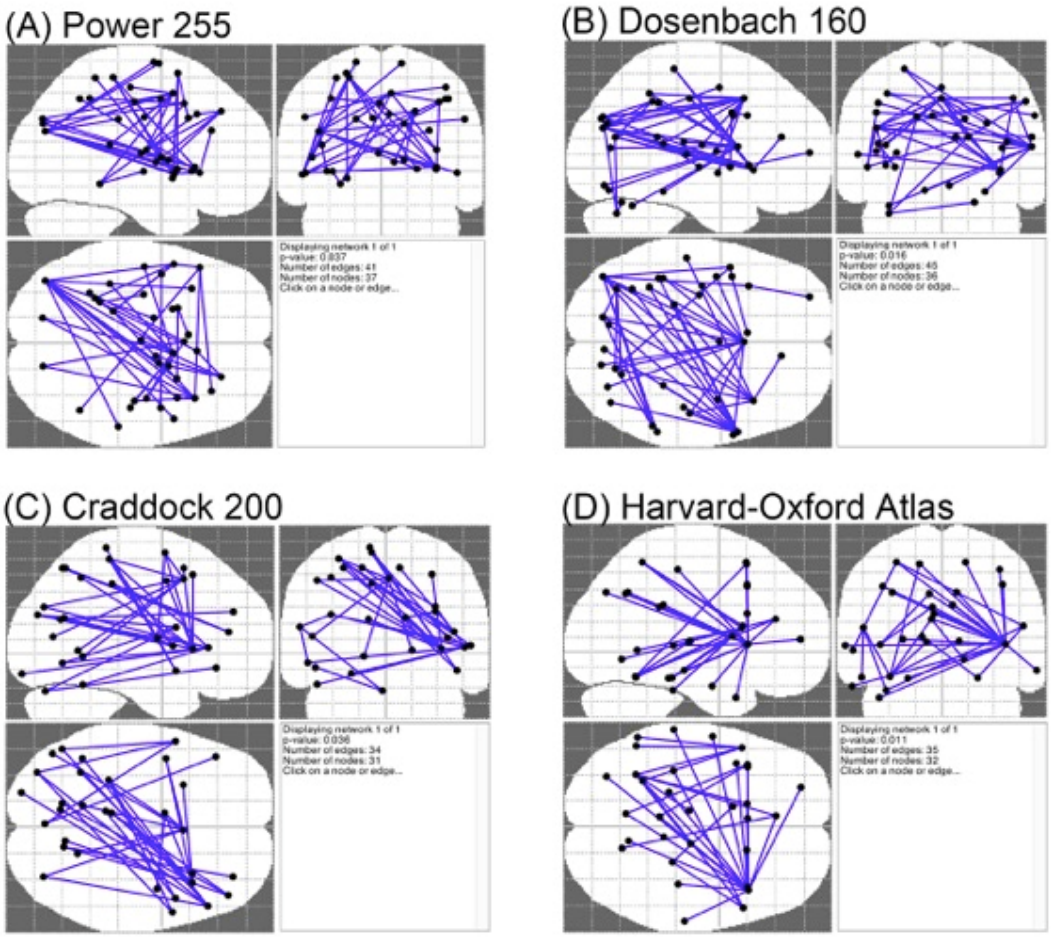

Supplementary Figure 1. *Changes in functional connectivity between adult ADHD and matched healthy controls across different brain parcellations.* The Network Based Statistics (NBS) showed stronger (generally stronger positive correlations, see Supplementary Table 3) functional connectivity in a single whole-brain network in ADHD compared to healthy controls. (A) 255 regions of interest parcellation (Power *et al.*, 2011). (B) 160 regions of interest parcellation (Dosenbach *et al.*, 2010). (C) 200 regions of interest parcellation (Craddock *et al.*, 2012). (D) the anatomical parcellation based on the Harvard-Oxford probabilistic cortical and subcortical atlases (www.fmrib.ox.ac.uk/fsl). Overall, the results obtained from different brain parcellations were similar.

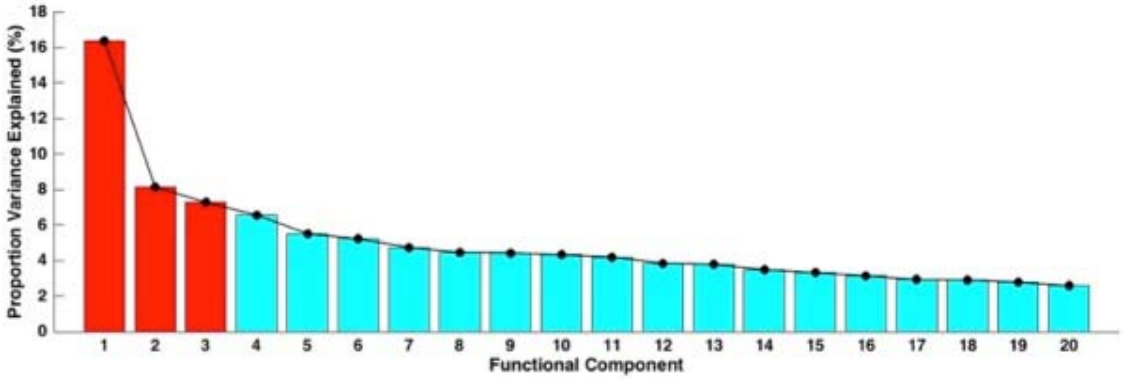

Supplementary Figure 2. *The proportion of variance explained by the eigenvectors defined by a principal component analysis on functional connectivity differences between ADHD and controls (derived from the network-based statistics).* The three eigenvectors (red) used in the canonical correlation analysis (CCA, see text) explained 31.83% of the total variance in between-groups connectivity. Including two extra eigenvectors allows to explain 43.90% of the variance. CCA based on both three and five eigenvectors yielded a similarly significant CCA mode.

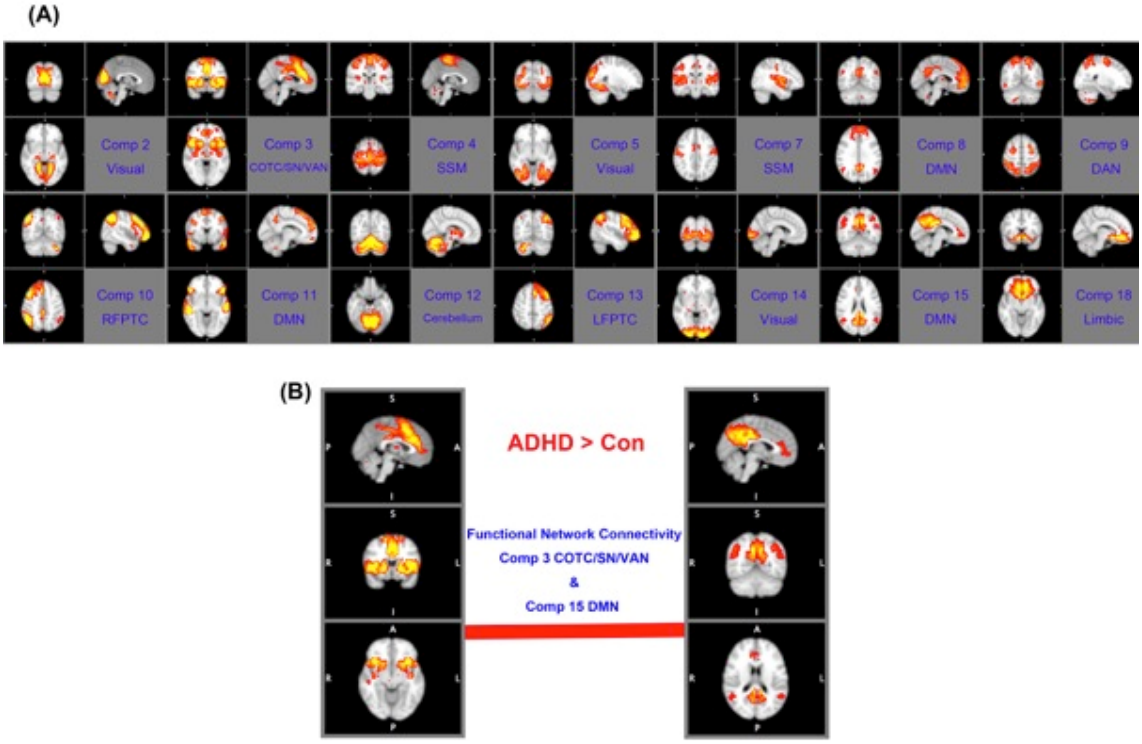

Supplementary Figure 3. *Independent component analysis (ICA) on neuroimaging data.* (A) Based on the group ICA, we identified 20 spatial components. The topology of 14 components related to recognized functional brain networks (Cocchi *et al.*, 2012b, Yeo *et al.*, 2011). These 14 components were used for the confirmatory functional network connectivity analysis (see text) (Jafri *et al.*, 2008). (B) Results from the functional network connectivity analysis. Relative to the controls, adults with ADHD exhibited a significantly increased positive interaction between the default-mode and cingulo-opercular/salience networks (false discovery rate corrected q=0.044).

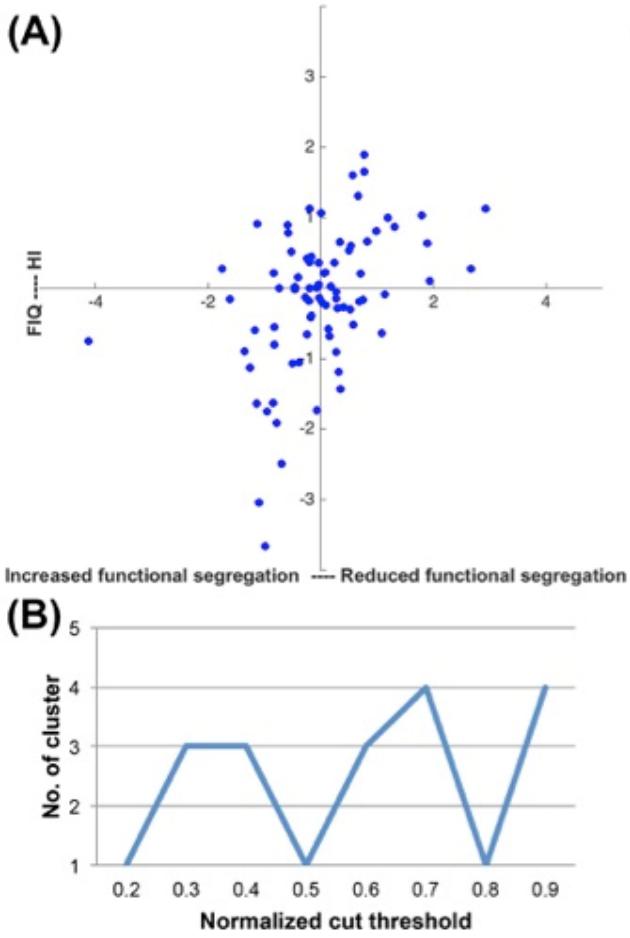

Supplementary Figure 4. *Test for ADHD categorical biotypes.* (A) K-means analysis failed to reveal valid clusters based on the individual associations between functional connectivity and behavior. The absence of clear clusters in the data is evident from visual inspection of the figure. (B) The number (No.) of clusters detected by the multi-view spectral clustering algorithm changed as a function of the preset cut threshold, indicating that no stable decomposition was achievable. Overall, results from these analyses provide compelling evidence for the absence of non-overlapping clusters in the data. FIQ=full-scale IQ; HI=hyperactivity-impulsivity.

4. References for Supplementary Materials

Abdi, H. & Williams, L. J. (2010). Principal component analysis. **2**, 433-459.

Asherson, P., Buitelaar, J., Faraone, S. V. & Rohde, L. A. (2016). Adult attention-deficit hyperactivity disorder: key conceptual issues. **3**, 568-578.

Beckmann, C. F. & Smith, S. M. (2004). Probabilistic independent component analysis for functional magnetic resonance imaging. **23**, 137-152.

Benjamini, Y. & Hochberg, Y. (1995). Controlling the false discovery rate: a practical and powerful approach to multiple testing. 289-300.

Birn, R. M., Molloy, E. K., Patriat, R., Parker, T., Meier, T. B., Kirk, G. R., Nair, V. A., Meyerand, M. E. & Prabhakaran, V. (2013). The effect of scan length on the reliability of resting-state fMRI connectivity estimates. **83**, 550-558.

Chang, L. R., Chiu, Y. N., Wu, Y. Y. & Gau, S. S. (2013). Father's parenting and father-child relationship among children and adolescents with attention-deficit/hyperactivity disorder. *Comprehensive psychiatry* **54**, 128-140.

Chao, C. Y., Gau, S. S., Mao, W. C., Shyu, J. F., Chen, Y. C. & Yeh, C. B. (2008). Relationship of attention-deficit-hyperactivity disorder symptoms, depressive/anxiety symptoms, and life quality in young men. *Psychiatry and clinical neurosciences* **62**, 421-426.

Chen, H., Li, K., Zhu, D., Jiang, X., Yuan, Y., Lv, P., Zhang, T., Guo, L., Shen, D. & Liu, T. (2013). Inferring group-wise consistent multimodal brain networks via multi-view spectral clustering. **32**, 1576-1586.

Cocchi, L., Harrison, B. J., Pujol, J., Harding, I. H., Fornito, A., Pantelis, C. & Yucel, M. (2012). Functional alterations of large-scale brain networks related to cognitive control in obsessive-compulsive disorder. **33**, 1089-1106.

Craddock, R. C., James, G. A., Holtzheimer, P. E., 3rd, Hu, X. P. & Mayberg, H. S. (2012). A whole brain fMRI atlas generated via spatially constrained spectral clustering. **33**, 1914-1928.

DiStefano, C., Zhu, M. & Mindrila, D. (2009). Understanding and using factor scores: Considerations for the applied researcher. **14**, 1-11.

Dolnicar, S. (2002). A review of unquestioned standards in using cluster analysis for data-driven market segmentation. In *CD Conference Proceedings of the Australian and New Zealand Marketing Academy Conference 2002 (ANZMAC 2002)*: Deakin University, Melbourne.

Dosenbach, N. U., Nardos, B., Cohen, A. L., Fair, D. A., Power, J. D., Church, J. A.,

Nelson, S. M., Wig, G. S., Vogel, A. C., Lessov-Schlaggar, C. N., Barnes, K. A., Dubis, J. W., Feczko, E., Coalson, R. S., Pruett, J. R., Jr., Barch, D. M., Petersen, S. E. & Schlaggar, B. L. (2010). Prediction of individual brain maturity using fMRI. **329**, 1358-1361.

Gau, S. F. & Soong, W. T. (1999). Psychiatric comorbidity of adolescents with sleep terrors or sleepwalking: a case-control study. **33**, 734-739.

Gau, S. S., Chong, M. Y., Chen, T. H. & Cheng, A. T. (2005). A 3-year panel study of mental disorders among adolescents in Taiwan. **162**, 1344-1350.

Gau, S. S., Kessler, R. C., Tseng, W. L., Wu, Y. Y., Chiu, Y. N., Yeh, C. B. & Hwu, H. G. (2007). Association between sleep problems and symptoms of attention-deficit/hyperactivity disorder in young adults. *Sleep* **30**, 195-201.

Gau, S. S., Shang, C. Y., Liu, S. K., Lin, C. H., Swanson, J. M., Liu, Y. C. & Tu, C. L. (2008). Psychometric properties of the Chinese version of the Swanson, Nolan, and Pelham, version IV scale - parent form. **17**, 35-44.

Hennig, C. (2008). Dissolution point and isolation robustness: robustness criteria for general cluster analysis methods. **99**, 1154-1176.

Huettel, S. A., Song, A. W. & McCarthy, G. (2008). *Functional magnetic resonance imaging*. Sinauer Associates: Sunderland.

Hyvarinen, A. (1999). Fast and robust fixed-point algorithms for independent component analysis. **10**, 626-634.

Jafri, M. J., Pearlson, G. D., Stevens, M. & Calhoun, V. D. (2008). A method for functional network connectivity among spatially independent resting-state components in schizophrenia. **39**, 1666-1681.

Kononenko, I. & Kukar, M. (2007). *Machine learning and data mining: introduction to principles and algorithms*. Horwood Publishing.

Kumar, A. & Daumé, H. (2011). A co-training approach for multi-view spectral clustering. In *Proceedings of the 28th International Conference on Machine Learning (ICML-11)*, pp. 393-400.

Kundu, P., Brenowitz, N. D., Voon, V., Worbe, Y., Vertes, P. E., Inati, S. J., Saad, Z. S., Bandettini, P. A. & Bullmore, E. T. (2013). Integrated strategy for improving functional connectivity mapping using multiecho fMRI. **110**, 16187-16192.

Kundu, P., Inati, S. J., Evans, J. W., Luh, W. M. & Bandettini, P. A. (2012). Differentiating BOLD and non-BOLD signals in fMRI time series using multi-echo EPI. **60**, 1759-1770.

Lombardo, M. V., Auyeung, B., Holt, R. J., Waldman, J., Ruigrok, A. N., Mooney, N.,

Bullmore, E. T., Baron-Cohen, S. & Kundu, P. (2016). Improving effect size estimation and statistical power with multi-echo fMRI and its impact on understanding the neural systems supporting mentalizing. **142**, 55-66.

Lv, J., Iraji, A., Ge, F., Zhao, S., Hu, X., Zhang, T., Han, J., Guo, L., Kou, Z. & Liu, T. (2016). Temporal Concatenated Sparse Coding of Resting State fMRI Data Reveal Network Interaction Changes in mTBI. In *International Conference on Medical Image Computing and Computer-Assisted Intervention*, pp. 46-54. Springer.

Ni, H. C., Lin, Y. J., Gau, S. S., Huang, H. C. & Yang, L. K. (2013a). An Open-Label, Randomized Trial of Methylphenidate and Atomoxetine Treatment in Adults With ADHD. *Journal of attention disorders*.

Ni, H. C., Shang, C. Y., Gau, S. S., Lin, Y. J., Huang, H. C. & Yang, L. K. (2013b). A head-to-head randomized clinical trial of methylphenidate and atomoxetine treatment for executive function in adults with attention-deficit hyperactivity disorder. *The international journal of neuropsychopharmacology* **16**, 1959-1973.

Orvaschel, H., Puig-Antich, J., Chambers, W., Tabrizi, M. A. & Johnson, R. (1982). Retrospective assessment of prepubertal major depression with the Kiddie-SADS-e. *Journal of the American Academy of Child Psychiatry* **21**, 392-397.

Power, J. D., Cohen, A. L., Nelson, S. M., Wig, G. S., Barnes, K. A., Church, J. A., Vogel, A. C., Laumann, T. O., Miezin, F. M., Schlaggar, B. L. & Petersen, S. E. (2011). Functional network organization of the human brain. **72**, 665-678.

Shi, J. & Malik, J. (2000). Normalized cuts and image segmentation. **22**, 888-905.

Smith, S. M., Fox, P. T., Miller, K. L., Glahn, D. C., Fox, P. M., Mackay, C. E., Filippini, N., Watkins, K. E., Toro, R., Laird, A. R. & Beckmann, C. F. (2009). Correspondence of the brain's functional architecture during activation and rest. **106**, 13040-13045.

Smith, S. M., Hyvarinen, A., Varoquaux, G., Miller, K. L. & Beckmann, C. F. (2014). Group-PCA for very large fMRI datasets. **101**, 738-749.

Smith, S. M., Nichols, T. E., Vidaurre, D., Winkler, A. M., Behrens, T. E., Glasser, M. F., Ugurbil, K., Barch, D. M., Van Essen, D. C. & Miller, K. L. (2015). A positive-negative mode of population covariation links brain connectivity, demographics and behavior. **18**, 1565-1567.

Swanson, J. M., Kraemer, H. C., Hinshaw, S. P., Arnold, L. E., Conners, C. K., Abikoff, H. B., Clevenger, W., Davies, M., Elliott, G. R., Greenhill, L. L., Hechtman, L., Hoza, B., Jensen, P. S., March, J. S., Newcorn, J. H., Owens, E. B., Pelham, W. E., Schiller, E.,

Severe, J. B., Simpson, S., Vitiello, B., Wells, K., Wigal, T. & Wu, M. (2001). Clinical relevance of the primary findings of the MTA: success rates based on severity of ADHD and ODD symptoms at the end of treatment. *Journal of the American Academy of Child and Adolescent Psychiatry* **40**, 168-179.

Takahashi, M., Goto, T., Takita, Y., Chung, S. K., Wang, Y. & Gau, S. S. (2014). Open-label, dose-titration tolerability study of atomoxetine hydrochloride in Korean, Chinese, and Taiwanese adults with attention-deficit/hyperactivity disorder. *Asia-Pacific psychiatry : official journal of the Pacific Rim College of Psychiatrists* **6**, 62-70.

Tao, H., Hou, C. & Yi, D. (2014). Multiple-view spectral embedded clustering using a co-training approach. In *Computer Engineering and Networking*, pp. 979-987. Springer.

Van Dijk, K. R., Hedden, T., Venkataraman, A., Evans, K. C., Lazar, S. W. & Buckner, R. L. (2010). Intrinsic functional connectivity as a tool for human connectomics: theory, properties, and optimization. **103**, 297-321.

Venkataraman, A., Van Dijk, K. R., Buckner, R. L. & Golland, P. (2009). Exploring Functional Connectivity in Fmri Via Clustering. **2009**, 441-444.

Yang, H. N., Tai, Y. M., Yang, L. K. & Gau, S. S. (2013). Prediction of childhood ADHD symptoms to quality of life in young adults: adult ADHD and anxiety/depression as mediators. *Research in developmental disabilities* **34**, 3168-3181.

Yeh, C. B., Gau, S. S., Kessler, R. C. & Wu, Y. Y. (2008). Psychometric properties of the Chinese version of the adult ADHD Self-report Scale. **17**, 45-54.

Yeo, B. T., Krienen, F. M., Sepulcre, J., Sabuncu, M. R., Lashkari, D., Hollinshead, M., Roffman, J. L., Smoller, J. W., Zollei, L., Polimeni, J. R., Fischl, B., Liu, H. & Buckner, R. L. (2011). The organization of the human cerebral cortex estimated by intrinsic functional connectivity. **106**, 1125-1165.